Controlled release of biological factors for endogenous progenitor cell migration and intervertebral disc extracellular matrix remodelling

Leslie Frapin, Johann Clouet, Claire Chédeville, Constantin Moraru, Edouard Samarut, Nina Henry, Manon André, Eric Bord, Boris Halgand, Julie Lesoeur, et al.

Controlled release of biological factors for endogenous progenitor cell migration and intervertebral disc extracellular matrix remodelling

Leslie Frapin[1,2], Johann Clouet[1,2,3,4], Claire Chédeville[1,2], Constantin Moraru[1,2,5], Edouard Samarut[1,2,5], Nina Henry[1,2], Manon André[1,2,6], Eric Bord[1,2,5], Boris Halgand[1,2,8], Julie Lesoeur[1,2,6], Marion Fusellier[1,2,7], Jérôme Guicheux[1,2,6,8*], Catherine Le Visage[1,2,*]

[1] Inserm, UMR 1229, RMeS, Regenerative Medicine and Skeleton, Université de Nantes, ONIRIS, Nantes, F-44042, France

[2] Université de Nantes, UFR Odontologie, Nantes, F-44042, France

[3] CHU Nantes, Pharmacie Centrale, PHU 11, Nantes, F-44093, France

[4] Université de Nantes, UFR Sciences Biologiques et Pharmaceutiques, Nantes, F-44035, France

[5] CHU Nantes, service de neurotraumatologie, PHU4 OTONN, Nantes, F-44093, France

[6] SC3M – "Electron Microscopy, Microcharacterization, and Functional Morphohistology Imaging" Core Facility, Structure Fédérative de Recherche François Bonamy, INSERM – UMS016, CNRS 3556, CHU Nantes, Université de Nantes, Nantes, Nantes, F-04402, France

[7] Department of Diagnostic Imaging, CRIP, National Veterinary School (ONIRIS), Nantes, F-44307, France

[8] CHU Nantes, PHU4 OTONN, Nantes, F-44093, France

* equally contributing/co-corresponding authors: jerome.guicheux@univ-nantes.fr; catherine.levisage@inserm.fr

ABSTRACT

The recent description of resident stem/progenitor cells in degenerated intervertebral discs (IVDs) supports the notion that their regenerative capacities could be harnessed to stimulate endogenous repair of the nucleus pulposus (NP). In this study, we developed a delivery system based on pullulan microbeads (PMBs) for sequential release of the chemokine CCL-5 to recruit these disc stem/progenitor cells to the NP tissue, followed by the release of the growth factors TGF-β1 and GDF-5 to induce the synthesis of a collagen type II- and aggrecan-rich extracellular matrix (ECM). Bioactivity of released CCL5 on human adipose-derived stem cells (hASCs), selected to mimic disc stem/progenitors, was demonstrated using a Transwell® chemotaxis assay. The regenerative effects of loaded PMBs were investigated in ex vivo spontaneously degenerated ovine IVDs. Fluorescent hASCs were seeded on the top cartilaginous endplates (CEPs); the degenerated NPs were injected with PMBs loaded with CCL5, TGF-β1, and GDF-5; and the IVDs were then cultured for 3, 7, and 28 days to allow for cell migration and disc regeneration. The PMBs exhibited sustained release of biological factors for 21 days. Ex vivo migration of seeded hASCs from the CEP toward the NP was demonstrated, with the cells migrating a significantly greater distance when loaded PMBs were injected (5.8 ± 1.3 mm vs. 3.5 ± 1.8 mm with no injection of PMBs). In ovine IVDs, the overall NP cellularity, the collagen type II and the aggrecan staining intensities, and the Tie2+ progenitor cell density in the NP were increased at day 28 compared to the control groups. Considered together, PMBs loaded with CCL5/TGF-β1/GDF-5 constitute an innovative and promising strategy for controlled release of growth factors to promote cell recruitment and extracellular matrix remodelling.

KEYWORDS

Disc disease; Ex vivo model; Chemokines; Microbeads, Regeneration; Cell recruitment

INTRODUCTION

Low back pain (LBP) is an ongoing major socio-economic problem in industrialized societies, affecting 80% of the world population at least once in their lifetime [1]. LBP is associated with repeated work absences and it represents one of the leading causes of severe disability and deterioration in the quality of life [2]. Intervertebral disc (IVD) degeneration is currently acknowledged to be one of the major causes of chronic LBP [3,4]. IVD is paramount for spine stability and mobility. The nucleus pulposus, which is the central part of the IVD, is gelatinous and hydrated, thereby allowing the IVD to resist compressive strains. The annulus fibrosus (AF), which surrounds the NP, offers elastic properties and resistance to tensile stresses. Finally, two cartilaginous endplates (CEPs) lie on either side of the IVD, forming a junction with the vertebral bodies while allowing the diffusion of oxygen, nutrients, and metabolic waste products [5]. These three specific structures of the IVD provide a suitable environment for absorption of spinal column impacts and they act as fibro-hydraulic shock absorbers [6,7]. Mechanical loading, trauma, and aging constitute the main risk factors for IVD degeneration. A pronounced decline in NP cell density combined with loss of the homeostasis balance leads to substantial deterioration of the quality and the quantity of the NP extracellular matrix (ECM) components, with a decrease in aggrecan and type II collagen fibres. This alteration could be due to abnormal and/or increased inflammatory and catabolic activities in particular, as evidenced by increased expression of IL-1β, -6, -8, TNF-α, MMPs, and ADAMTSs [8,9]. These biological impairments orchestrate structural alterations that affect the mechanical properties of the IVD, thereby often giving rise to low back pain. This degenerative cascade leads to a vicious circle that amplifies the IVD degeneration and it prevents natural repair processes from taking place [6,10]. The currently available treatments for discogenic LBP are focused on pain relief via pharmacological approaches or invasive surgical procedures in severe and resistant LBP cases, such as spine fusion or disc replacement. Although these surgical procedures have been shown to have a degree of clinical efficacy, particularly in terms of pain relief, they are, however, highly invasive and they risk inducing accelerated degeneration of adjacent discs as well as disruption of spine biomechanics, particularly with spine fusion. Moreover, they do not address the underlying pathogenic mechanisms of IVD degeneration, nor do they allow restoration of the biological integrity and function of IVDs [11].

In recent years, regenerative medicine approaches have been described as a promising option to stop or even to reverse degenerative disc disease (DDD) [12]. Among these approaches, the aim of cell therapies is to transplant exogenous cells to repopulate the degenerated NP and to reinitiate the anabolic IVD machinery, thereby leading to the synthesis of an adequate ECM that could contribute to restoration of the IVD height. In particular, mesenchymal stem/stromal cells (MSCs) have been studied extensively as a promising source of cells [13]. Preclinical trials involving the injection of MSCs have yielded positive results, with an increase in type II collagen fibre synthesis. Clinical trials in humans have revealed significant pain relief and improvement of the quality of life of patients, albeit with very few signs of IVD regeneration [14]. Thus, a number of studies have suggested therapeutic in vitro manipulation of MSCs prior to their injection, in order to generate NP-like cells, using growth factor-driven differentiation protocols [15,16]. Co-culture experiments have also been performed to evaluate the effects of injected MSCs on resident NP cells [17,18]. However, the injection of exogenous cells suffers from a major

drawback, mainly due to the limited survival of cells after their injection into the harsh NP microenvironment [19,20]. Indeed, degenerated IVDs represent a hostile microenvironment, with a high osmotic pressure, acidic pH, low nutrient availability, and hypoxic conditions, as well as degenerative inflammatory and catabolic events [5]. In addition, osteophyte formation following MSC injection has been reported, and technological and regulatory restrictions have hampered the transfer of cell-based therapies into patients [21].

Recently, stem/progenitor cells have been reported to be present in healthy and degenerated IVD tissues from human and various other mammalian species [22–24]. Potential migration within the disc tissue has been suggested, as well as the existence of a migration route connecting the CEP, the AF, and the NP [25]. These disc stem/progenitor cells resemble MSCs as they express typical MSCs markers (CD90, CD105, CD45, and STRO1), and they can be differentiated in vitro into osteocytes and chondrocytes [11,26,27]. Interestingly, comparative studies of these disc stem/progenitor cells isolated from CEPs, the AF, and the NP have demonstrated the superiority of CEP-stem cells in terms of their capacity to migrate in vitro [28,29]. On the other hand, Tie2-positive progenitor cells have also been described in mouse, bovine, and human NP as potential sources of regenerative cells [30]. In this context, these endogenous disc stem/progenitor cells constitute a promising alternative to the use of exogenous stem cells for IVD regenerative strategies [31]. However, such endogenous repair strategies face the challenge of recruiting disc stem/progenitor cells from the periphery of the IVD and the CEPs, where they are most abundant, toward the degenerated NP. Interestingly, ex vivo studies performed on bovine IVDs cultured under degenerative conditions, have demonstrated overexpression of chemokines known to specifically recruit MSCs [32,33]. These results suggest that a natural mechanism of endogenous healing occurs in degenerative IVDs, but this may not be sufficient to allow for full restoration of disc homeostasis [10]. This low regenerative capacity could be due to the IVD's avascularity, which limits the availability of nutrients and oxygen [5].

Chemokines and growth factors act as mediators of healing processes and they represent potential molecular targets to stimulate and guide regenerative mechanisms. Chemokine (CC-motif) ligand 5 (CCL5, also called Regulated upon Activation, Normal T cell Expressed, and Secreted, RANTES) recruits a substantial number of cells, including bone marrow mesenchymal stem cells (BM-MSCs) that express its specific membrane receptor CCR1/3/5 [34,35]. In the IVD context, CCL5 is secreted by disc cells, and CCL-5 receptors are expressed on the surface of AF and NP cells, thus suggesting that CCL5 could play a role in the IVD healing process [33]. Interestingly, physiological expression of CCL5 is upregulated under degenerative conditions [33,36,37]. Moreover, in patients, systemic CCL5 has been associated with discogenic back pain and moderate/severe lumbar disc degeneration, thus suggesting that CCL5 could be considered to be a biomarker for the diagnosis and monitoring of disc degeneration [38–40]. On the other hand, the growth factors TGF-β1 and GDF-5, both essential factors for IVD embryonic development, have been evaluated as therapeutic targets [41]. GDF-5 is physiologically present in IVD tissue and it participates in disc homeostasis by increasing type II collagen fibre and aggrecan synthesis by NP cells, which are also called nucleopulpocytes (NPCy) [42,43]. TGF-β1 induces upregulation of COL2A1 and ACAN gene expression in NPCy in vitro [44,45]. Of particular interest, we have demonstrated a synergistic role of these factors in the induction of nucleopulpogenic differentiation of human adipose stem cells (hASCs) after 28

days of in vitro culture, as evidenced by the synthesis of ECM rich in sulphated glycosaminoglycans (GAGs) and type II collagen fibres, and expression of specific NPCy markers, such as CD24, PAX1, and OVOS2 [46].

Biological factors are particularly prone to degradation in vivo, and their protection by biomaterials is an option to enable a sustained therapeutic effect with a single injection into the IVD [12,47]. A large panel of biomaterials, composed of natural or synthetic polymers, have been combined with biological factors [48]. Among these, polysaccharide microparticles have been studied for encapsulation of CCL5, TGF-β1, and GDF-5 [49,50]. Such microparticles have been prepared from pullulan, which is a linear polymer of glucose units that has already been approved by the Food and Drug Administration (FDA) and widely used in the food, pharmaceutical, and cosmetics industries [51–53]. We have previously studied these microbeads, particularly as a TGF-β1 and GDF-5 delivery system, with 27% and 100% release over 21 days, respectively, and maintenance of their biological activity in terms of SMAD-mediated phosphorylation pathways has been demonstrated in vitro [49].

In this context, the objective of the present study was to develop a delivery system composed of pullulan microbeads (PMBs) that could i) deliver CCL5 to recruit disc stem/progenitor cells, and ii) release a TGF-β1 and GDF-5 synergistic cocktail to stimulate the synthesis of an NP-like ECM. Since disc stem/progenitor cells, which are the cells ultimately targeted by an endogenous IVD regenerative strategy, are only present in small numbers and are difficult to isolate, we used hASCs as a substitute. This approach based on the use of model cells has been previously reported in several endogenous IVD repair studies [32,54–56]. We characterised the CCL5 adsorption and release kinetics, and we assessed the stimulatory effect of CCL5 on hASCs migration in vitro. Finally, we investigated the ex vivo effect of the injection of CCL5, TGF-β1, and GDF-5 PMBs in a degenerated IVD model in sheep by analysis of cell migration and tissue responses.

MATERIALS AND METHODS

FITC-Pullulan microbeads (PMBs)

First, pullulan (200 000 g/mol, Hayashibara Inc., Japan) was labelled with fluorescein isothiocyanate isomer I (FITC) (Sigma Aldrich, St Louis, MO, USA), as previously described [49]. FITC-pullulan (10 mg), combined with unlabelled pullulan (6 g), was dissolved in 20 mL of distilled water, under magnetic stirring, until a homogenous, viscous solution was obtained. Microbeads were then obtained using a combined emulsion/cross-linking process. Briefly, three 3 mL syringes were prepared in parallel with (1) 2.5 g of FITC-pullulan solution, (2) 250 µL of 10 M NaOH solution, and (3) 250 µL of 90% w/v sodium trimetaphosphate (Sigma Aldrich, St Louis, MO, USA) [57]. In parallel, 75 mL of rapeseed oil was placed in a 150 mL beaker and stirred for 30 minutes at room temperature. The contents of syringes (1) and (2) were then mixed using a Luer-lock connection, after which syringe (3) was connected to add the crosslinking agent. The resulting mixture was then quickly injected, within 30 seconds, using an 18G needle, into the oil phase under stirring at 450 rpm. The water/oil emulsion was then incubated at 37 °C for 90 minutes under magnetic stirring to allow for chemical cross-linking and microbead formation. The beads were then subjected to successive washing steps with PBS pH 7.4 (Sigma Aldrich, St Louis, MO, USA), followed by solutions of sodium dodecyl sulphate (0·008% w/v, Sigma Aldrich, St Louis, MO, USA) and then NaCl (0.0025%, Sigma Aldrich, MO, USA). The PMBs were then filtered using a blood transfusion set (mesh aperture 200 µm, CareFusion, San Diego, CA, USA), freeze-dried, and stored at room temperature until use. All of the formulated PMB batches were then pooled to obtain a single batch.

The PMBs were observed by fluorescence microscopy (DM IL LED Fluo, Leica, Germany) to visualize their shape before and after freeze-drying. Their size was measured using particle size analysis (Mastersizer 3000 Laser, Malvern Instruments, UK). For each FITC-PMB batch, 5 measurements were performed using 30 mg of freeze-dried PMBs rehydrated in PBS.

PMB loading with CCL5 chemokine

All of the loading and release experiments were performed using 20 mg of freeze-dried PMBs, corresponding to 800 000 microbeads, that had been decontaminated by exposure to UV light for 30 minutes. Three concentrations (1, 2, and 4 µg/mL in PBS/BSA) of human CCL5 (# 278-RN, R&D Systems Inc., Minneapolis, MN, USA) were prepared in filter-sterilized PBS pH 7.4 (Thermo Fisher Scientific, St Aubin, France), containing 1% w/v of bovine serum albumin (BSA, Sigma Aldrich, St Louis, MO, USA), as the buffer solution. The PMBs were suspended in 500 µL of chemokine solution and loading was performed by adsorption at 4 °C under rotary stirring on a Mini LabRoller™ Dual Format Rotator (Labnet) for 24 hours. Unloaded PMBs were prepared in parallel by omission of the chemokines from the process. To remove unloaded chemokines, the samples were centrifuged at 5 000 rpm for 10 minutes, at 4 °C. The supernatants were then retrieved for ELISA assays (# 278-05, Duoset® kits, R&D Systems Inc., Minneapolis, MN, USA) to measure the amount of unloaded CCL5 and to calculate the amount of adsorbed chemokines and the adsorption efficacy. The experiments were performed in triplicate for each condition.

Loading of PMBs with growth factors

The loading was performed as previously described [49], using 20 mg of freeze-dried PMBs, corresponding to 800 000 microbeads, that had been decontaminated and suspended in 500 µL of 1.2 µg/mL human TGF-β1 (# 100-21, 50 µg/mL, PeproTech, Neuilly-Sur-Seine, France) or 2.4 µg/mL of human GDF-5 (# 120-01, 100 µg/mL, PeproTech, Neuilly-Sur-Seine, France) solution prepared in filter-sterilized PBS/BSA. The loading was performed by adsorption at 4 °C under rotary stirring on a Mini LabRoller™ Dual Format Rotator (Labnet) for 24 hours.

Visualization of adsorbed chemokines

Chemokine-loaded PMBs, and unloaded PMBs, were washed in PBS immediately after adsorption and then fixed in 4% w/v paraformaldehyde (PFA) for 10 minutes at room temperature. After three wash steps with PBS, the PMBs were incubated overnight at 4 °C with human CCL5 (# AF-278-NA, R&D Systems Inc., Minneapolis, MN, USA) at 10 µg/mL in PBS1X. Samples were then incubated for 1 h at room temperature with a secondary antibody (1:1 000 anti-goat IgG Alexa Fluor® 577 nm; NorthernLights™, R&D Systems Inc., Minneapolis, MN, USA). For all of the incubation steps, the samples were rotary stirred on a Mini LabRoller™ Dual Format Rotator (Labnet). The labelled PMBs were then mounted on glass slides with Prolong® (Molecular probes®, Life Technologies, USA) and observed by fluorescence confocal microscopy (A1RS, Nikon, Champigny-sur-Marne, France). The acquired images were then processed with ImageJ software. The experiments were performed in triplicate for each condition.

In vitro release of chemokines from PMBs

Chemokine-loaded PMBs were suspended in 500 µL of PBS/BSA at 37 °C for 21 days, under rotary stirring. At 1 h, 2 h, 4 h, 8 h, 24 h, 48 h, 72 h, 4 days, 7 days, 14 days, and 21 days, PMBs were centrifuged at 5 000 rpm for 10 minutes at 4 °C and the supernatants were collected and replaced with fresh PBS/BSA. The collected supernatants were used for ELISA assays to evaluate the amount of released CCL5 at each time point. The experiments were performed in triplicate for each condition and each time point. For all of the subsequent experiments, the loaded PMBs were prepared using chemokine solutions at 4 µg/mL.

In vitro bioactivity of chemokines

Adipose stem cell isolation and culture

Human adipose-derived stromal cells (ASCs) were collected from lipoaspirates harvested from 7 adult donors (33-64 years of age) who had provided their informed consent (Supplementary Table 1). Adipose tissues were enzymatically digested and human ASCs were isolated by density gradient centrifugation and adherence to tissue culture plastic as previously described [46,58] and expanded with complete culture medium (high-glucose Dulbecco's modified Eagle's medium DMEM, Gibco, Life Technologies, Paisley, UK) supplemented with 10% w/w foetal calf serum (FCS) (Dominique Dutscher, France), 1% w/w Penicillin/Streptomycin (P/S), and 0.1% w/w fungizone. The human ASCs were used at no more than passage 4.

In vitro migration assay

Human ASC migration assays were performed in 24-well plates combined with Transwell inserts with an 8-µm pore polycarbonate membrane (Corning, 3422, Kennebunk ME, USA). The cells were deprived of serum the day before the experiment, detached with trypsin, and then suspended in serum-free culture medium supplemented with 0.1% BSA w/v. The cells (250 000 cells) were seeded on the top of the inserts (200 µL). Aliquots of CCL5 solution (250 ng/mL) were prepared in serum-free culture medium supplemented with 0.1% w/v of BSA and added to the bottom chamber of the wells (500 µL). Control experiments were performed by omission of the chemokines. After 4 h of incubation at 37 °C in a 20% O_2, 5% CO_2 atmosphere, the cells that remained on top of the inserts were removed using a cotton swab, while those that migrated to the lower side of the insert were fixed with cold methanol (VWR Prolabo Chemicals, Fontenay-sous-Bois, France) and stained with a 0.1% w/v crystal violet solution (Sigma Aldrich, St Louis, MO, USA). After observing the stained cells that had migrated using light microscopy, crystal violet was solubilized in 500 µL of acetic acid (Merck Millipore, Darmstadt, Germany, 1% v/v). The absorbance was quantified at 595 nm (PerkinElmer) and the number of cells that had migrated was calculated from a standard curve.

In a further experiment, the migration assays were performed by replacing the chemokine solutions with PMBs loaded with CCL5 to evaluate the bioactivity of the chemokine released over time. Time-course in vitro migration assays were performed with 250 000 cells/insert and a migration duration of 4 hours. First, chemokine-loaded CCL5/PMBs, prepared in serum-free culture medium supplemented with 0.1% w/v of BSA, were added to 24-well plates (500 µL) and incubated at 37 °C. At each release time point (0 h, 4h, 24h, 48 h, 72 h, and day 7), human ASCs were seeded on the top of a Transwell insert (250 000 cells/insert) as previously described, and the migration assay was performed with cells in the presence of the CCL5/PMBs for 4 hours at 37 °C. The inserts were then removed and the cells that had migrated were analysed by staining with crystal violet, while the 24-well plates containing the loaded PMBs were reincubated at 37 °C for further chemokine release and additional analyses. Controls experiments were performed with unloaded PMBs and free-chemokine solutions. The experiments were performed in triplicate, with cells from 4 human donors (D, E, F, and G).

Ovine IVD isolation

IVDs were collected from 10 sheep that were between 1 and 7 years old (Vendée breed, GAEC HEAS, Les Rabelais, Ligné, France) in the accredited Centre of Research and Pre-Clinical Investigations (ONIRIS, National Veterinary School of Nantes). The sheep received a bolus hypocoagulant dose of heparin (50 IU/kg) and were euthanized with an overdose of barbiturates (60 mg/kg) in accordance with the current best practices and legislation (European Directive 2010/63/EU). Post-euthanasia medullar MRI of the thoracolumbar sheep spines were performed to obtain T2-weighted images (TE: 86 ms, TR: 3,000 ms; slice thickness: 3 mm), using a 1.5 T MRI scanner (Magnetom Essenza®, Siemens Medical Solutions, Erlangen, Germany) [59]. Post-euthanasia X-ray imaging was conducted using a radiography machine (Convix 80® generator and Universix 120 table) from Picker International (Uniontown, Ohio, USA), to obtain coronal and sagittal plane radiographs of the sheep lumbar spines, with a collimator-to-film distance of 100 cm, an exposure of 100 mAs, and a penetration power of 48 kVp. Osirix

software® (3.9, Osirix Foundation, Geneva, Switzerland) was used to analyse the X-ray and the MRI images, and each lumbar IVD was analysed using the Pfirrmann grading system [60] by two neurosurgeons at the Nantes hospital. After extraction of the thoracolumbar spine via a posterior approach, under aseptic conditions, the IVDs were individually isolated by removal of the vertebral bodies with an oscillating saw without damaging the cartilaginous endplates, as previously described for a bovine caudal model [54,61].

Ovine IVD ex vivo culture

Isolated IVDs were cultured in 30 mL of IVD culture medium composed of high-glucose DMEM, 2% FCS, P/S 1% v/v, fungizone 0.1% v/v, ITS 1.25% v/v, ascorbate-2-phosphate 1% w/v, and non-essential amino-acids 1% w/v, at 37 °C in a 20% O_2 and 5% CO_2 atmosphere. To evaluate the feasibility of long-term culture of healthy ovine IVDs, a preliminary study with isolated lumbar IVDs from 4 young sheep (1-year-old, Pfirrmann grade 1), cultured for 7, 14, and 21 days, was performed. To assess the feasibility of injecting PMBs, the IVDs were injected at day 0 with PMBs (0.8% w/w suspension in PBS) via a transannular pathway and a 23G needle connected to a 1-mL syringe (injected volume 200 µL) and cultured for 7, 14, and 21 days. The IVDs were processed for histological sectioning, after one of the cartilaginous endplates was removed with a scalpel. The IVDs were frozen for 3 minutes in isopentane/dry ice and then embedded in Super Cryoembedding Medium (SCEM) (Section-lab, Hiroshima, Japan), frozen again in isopentane/dry ice, and finally stored at -80 °C until further use. The frozen IVDs were sectioned (7-10 µm) with a CryoStar NX70® cryostat (Thermo Fisher Scientific, Waltham, Massachusetts, USA) in the axial orientation, starting from the side without a CEP. The frozen IVD sections were stained with Alcian blue and haematoxylin/eosin/saffron (HES) or used for cell metabolism activity analysis using a Lactate Dehydrogenase/Ethidium Homodimer (LDH/EtH) staining protocol. Briefly, frozen IVD sections were first incubated with 1 µg/mL EtH (Sigma Aldrich, St Louis, MO, USA) for 15 minutes at room temperature and then with a freshly prepared LDH solution (2 mM Gly-Gly buffer at pH 8·0 containing 40% Polypep, 5.4 mg/ml lactic acid, 1.75 mg/ml β-nicotinamide adenine dinucleotide hydrate, and 3 mg/mL nitrotetrazolium blue chloride (NBT)) for 3 h at 37 °C. The stained sections were then rinsed with distilled water at 50 °C and fixed with 4% PFA for 5 minutes. The sections were mounted on glass slides with Prolong® (Molecular probes®, Life Technologies, USA) and observed both by brightfield and fluorescence (excitation/emission 528/617 nm) microscopy using a slide scanner (NanoZoomer®, Hamamatsu Photonics, Hamamatsu, Japan). Image analysis was performed with NDP.view2 software® (Hamamatsu Photonics). The results are expressed as the percentage of metabolically active cells (labelled by LDH) in relation to the total number of cells observed in the NP and the AF.

Ex vivo bioactivity of PMBs loaded with chemokine and growth factors

To evaluate the activity of our sequential delivery system on a cellularized IVD microenvironment, CCL5/PMBs, TGF-β1/PMBs, and GDF-5/PMBs were injected into the NP of an ex vivo IVD via a transannular pathway. hASCs were then seeded on the top cartilaginous endplate (**Fig. 6**). Briefly, 200 µL of loaded PMBs, containing 320 000 PMBs adsorbed with 800 ng of CCL5, 25 000 PMBs adsorbed with 600 ng of TGF-β1, and 25 000 PMBs adsorbed with 1 200 ng of GDF-5, were injected via a 23G needle connected to a 1-mL Hamilton syringe. The injection was

performed by applying a constant pressure and by pausing before removal of the needle to avoid reflux. The injected IVDs were then incubated for 2 hours in 30 mL of IVD culture medium at 37 °C, in a 20% O_2 and 5% CO_2 atmosphere. The culture medium was then removed and human ASCs (500 000 of cells in 100 µL, passage 1-3) were seeded on the top cartilaginous endplate. The IVDs were then incubated for 30 minutes before adding 30 mL of culture medium. Before injection, the human ASCs were freshly labelled with Vybrant™ Dil cell-labelling solution (#V-22888, Molecular Probes, USA), according to the supplier's guidelines. The culture medium was replaced every 2-3 days. The disc height was measured with callipers each time the medium was changed and the IVDs were carefully kept in the same orientation so that the seeded top endplate remained upright throughout the study. Control experiments with intact IVDs, IVDs injected only with loaded PMBs, and non-injected IVDs seeded with labelled human ASCs were performed. The IVDs were cultured for 3, 7, and 28 days for all conditions. Overall, 3 donors of human ASCs (D, E, and G) were used, and the IVDs were isolated from 6 sheep (3-7 years old) that had Pfirrmann grade 2 or 3 lumbar IVDs (**Fig. 6**).

Analysis of cell recruitment and regeneration in ex vivo ovine IVDs

At each time point, ex vivo IVDs were processed for histological analysis, with fixation in 4% PFA for 5 days, followed by decalcification (Shandon TBD-2™ Decalcifier, Thermo Fisher Scientific, Cheshire, UK) for 3 weeks and a post-fixation step, after abundant rinsing, in 4% PFA for 24 hours. All of the IVDs were then frozen and cryosectioned, as previously described, in the coronal orientation, starting from the posterior arch. To evaluate cell migration, the 18 IVDs seeded with hASCs were sectioned at 5 levels, separated from each other by 500 µm, while 18 other IVDs (intact- and loaded-PMB groups) were sectioned at 2 levels, separated from each other by 2 cm, for evaluation of the ECM. The frozen IVD sections were either directly mounted in Prolong® (Molecular probes®, Life Technologies, USA) to observe the localization of labelled human ASCs, or they were subjected to histological staining with Alcian blue, HES, and Masson's trichrome, or processed for immunohistochemical staining (**Fig.6**).

For immunostaining, frozen sections were incubated with chondroïtinase ABC (# C2905, Sigma Aldrich, St Louis, MO, USA) or 0.1% trypsin (# T9935, Sigma Aldrich, St Louis, MO, USA) or proteinase K (# P6556, Sigma Aldrich, St Louis, USA), for 30 minutes, and then with 3% v/v H_2O_2 (Sigma Aldrich, St Louis, MO, USA) to inactivate internal peroxidases. After blocking with 10% w/w goat serum in 4% w/w BSA (# A9647, Sigma Aldrich, St Louis, MO, USA,) for 30 minutes, the sections were incubated in the various primary antibody solutions (prepared in 0.1% v/v Triton and 4% w/v BSA) overnight at 4 °C. The primary antibodies were directed against: type I collagen (1:250 diluted ab138492, anti-human, Abcam, Cambridge, UK), type II collagen (1:100 diluted # 631701, anti-human, MP Biomedicals, France), Aggrecan (1:100 diluted ab3778, anti-human, Abcam, Cambridge, UK), and Tie2 (1:100 dilution, anti-sheep, CliniSciences, Nanterre, France). The sections were then incubated with a secondary antibody (biotinylated goat anti-mouse secondary antibody (1:500 diluted E0433, Dako, Agilent Technologies, Les Ulis, France,) for aggrecan or anti-rabbit secondary antibody (1:300 diluted E0432, Dako, Agilent Technologies, Les Ulis, France) for type I and II collagen and Tie2 for 1 h at room temperature. Following horseradish peroxidase-conjugated streptavidin amplification (1:400 dilution, Dako, Demark), the sections were developed with

diaminobenzidine (DAB kit, GBI Labs, CO2-12, USA) for 1 minute and counterstained with haematoxylin for 30 seconds.

The unstained and the stained sections were observed by brightfield and fluorescence microscopy using a slide scanner under (NanoZoomer®, Hamamatsu Photonics, Hamamatsu, Japan), and image analysis was performed with NDP.view2 software® (Hamamatsu Photonics) and ImageJ software. The cells identified in the NP that had migrated were counted using ImageJ software and the results are expressed as the mean value of the number of cells that migrated per section, with 5 sections (each separated by 500 µm) analysed per disc and per time point. The maximum migration distance from the endplate to the NP was measured using NDP.scan software. For each section, time point, and donor, the results are presented as the mean value of 3 measurements performed on a single section.

Statistical analysis

All of the results are presented as means ± SD. The statistical analyses were performed using GraphPad Prism 5.0® software (GraphPad, San Diego, California, USA). Statistical significance was determined using one-way ANOVA or two-way ANOVA followed by a Bonferroni's post-test for multiple group comparisons. Statistical significance was set at $p < 0.05$. Unless otherwise stated, the experiments were repeated at least three times.

RESULTS

Pullulan microbeads (PMBs) for chemokine adsorption and release

PMBs were successfully obtained by a water/oil emulsification process combined with a chemical crosslinking step during which phosphate bonds between the -OH groups of the pullulan chains are created, as described previously [49]. To perform the loading with biological factors, freeze-dried PMBs were rehydrated with CCL5 at three different loading concentrations (1, 2, and 4 µg/mL) and incubated at 4 °C for 24 hours. The loaded PMBs exhibited a spherical morphology and a mean size of 95.4 ± 0.5 µm (90% of the particle population had a diameter of less than 184 µm) (data not shown) [49]. ELISA assays performed on the supernatants obtained after centrifugation did not detect CCL5, thus indicating a 100% loading efficiency for this chemokine (data not shown). The absorption of the CCL5 on the PMBs was evidenced using red fluorescently labelled specific antibodies (**Fig. 1**). CCL5 adsorption was confirmed at all three of the tested concentrations, while the unloaded PMBs incubated with PBS did not exhibit any red fluorescence (**Fig. 1**).

The release of CCL5 into PBS supplemented with 1% w/v BSA was then studied for 21 days at 37 °C, with ELISA assays performed at each time point on the supernatants collected after centrifugation. Macroscopic observations at the end of the release experiment did not provide any evidence of degradation of the PMBs (data not shown). The results for the cumulative amount of CCL5 released over time are presented in **Fig. 1**. Overall, sustained delivery of adsorbed chemokine was observed for 21 days, at all initial loading concentrations. The PMBs/CCL5 (initial concentration of 4 µg/mL) exhibited an initial burst release during the first 24 h, with a release rate of 43 ng/h, followed by a continuous release of 0.07 ng/h. A similar profile was observed for the PMBs/CCL5 loaded at initial concentrations of 1 µg/mL and 2 µg/mL. At day 21, 85%, 99%, and 99% of the adsorbed CCL5 were released from PMBs loaded with initial concentrations of 1, 2, and 4 µg/mL, respectively.

In vitro migration assay

We then evaluated the ability of free and released chemokines to stimulate the migration of human adipose-derived stem cells (hASCs), which were used to mimic the endogenous progenitors, by means of a Transwell insert. We analysed the migratory effect of CCL5 (250 ng/mL in DMEM/BSA) on human ASCs, with experiments performed in triplicate on 3 donors (donors A, B, and C) (**Fig. 2**). Representative microscopic images of the lower side of the inserts, with cells stained with crystal violet, revealed that only a small number of the untreated cells, i.e., exposed to DMEM/BSA, had undergone spontaneous migration (**Fig. 2A**, left image), whereas numerous cells treated with CCL5 (**Fig. 2A**, right image) had migrated as they were detected on the lower side of the porous membrane. Quantitative analysis of the migration is presented as a migration fold increase for each donor (Fig. 2A, lower panel), compared to their own control group (untreated cells). We observed a striking degree of inter-donor variability, with migration of the cells from donor B barely enhanced by incubation with CCL5, while migration of the cells from donors A and C was increased 3.1- and 4.2-fold, respectively, in the presence of CCL5.

In a further experiment, we evaluated the chemokine recruitment activity over time by incubation of CCL5 solutions (at 4 µg/mL) or PMBs previously loaded with CCL5 (loading concentration 4 µg/mL) at 37 °C for up to 7 days using cells from four additional donors (D, E, F, and G). At specific time points (fresh solution or suspension, 4 h, 24 h, 48 h, 72 h, and 7 days of incubation), human ASCs were seeded on Transwell inserts (with 250 000 cells/insert) and a migration assay was then performed for 4 hours with cells in the presence of previously incubated free chemokines or released chemokines. The results are expressed as the fold increase compared to untreated cells or cells treated with unloaded PMBs (pooled for all donors D, E, F, and G) at each time point. For free CCL5 (**Fig. 2B**, left panel), a decreasing trend in activity over time was observed, with a 4.1-fold increase in migration with a fresh solution compared to untreated cells, and reduced migration after only 4 hours of incubation at 37 °C (fold increase of 1.4). No effect on the in vitro migration of human ASCs was observed after 72 hours or after 7 days. By contrast, PMBs loaded with CCL5 exerted an increased migratory effect on human ASCs that peaked at 24 hours (**Fig. 2B**, right panel). The results are expressed as the fold increase compared to cells treated with unloaded PMBs at the same time points (fresh suspension of PMBs, 4 h, 24 h, 48 h, 72 h, and 7 days of incubation). We observed an increase in the migratory effect on ASCs after 4 hours and 24 hours of incubation (fold increase of 1.6 and 2.0, respectively), and no migration was discernible when the CCL5/PMBs were incubated for 7 days before the migration assay. It is worth noting that pooled results from four human donors indicated no significant differences. To overcome the inherent inter-donor variation, we increased the number of in vitro experiments and we confirmed that a significant increase in migration was achieved with released CCL5 for three out of four cell donors. Moreover, similar bioactivity profiles were obtained with all four donors, with a maximum level of migration obtained with PMBs incubated for 4 h to 48 h (**Fig. 2C**).

Ex vivo lumbar ovine IVD long-term organ culture

We next investigated the feasibility of long-term organ culture with lumbar IVDs isolated from four sheep. Harvested IVDs (**Fig. 3A**) were cultured for 21 days and their structural integrity was analysed on histological sections stained with Alcian blue and HES. While a decrease in the Alcian blue staining intensity in the NP at day 21 was observed compared to day 0, there was no obvious alteration of the tissue cellularity on the HES sections. These data collectively show that we have, for the first time, successfully implemented an ex vivo culture model of ovine lumbar IVD that is able to maintain its cellular and histological organization for at least 3 weeks.

By using this model, we then tested whether PMBs suspended in PBS can be injected intradiscally. IVDs were hence injected at day 0 with PMBs (0.8% (w/w) suspension in PBS, injected volume 200 µL), via a trans-annular route and a 23G needle (n=8 discs), to estimate the impact of this injection on long-term IVD organ culture (**Fig. 3B**). At each time point (day 0, 7, 14, and 21), the discs were cryosectioned and negatively charged PMBs were visualized on Alcian blue sections as dark blue dots, as indicated by black arrows.

To further address whether this transannular injection of PMBs may affect IVD integrity during the course of culture, histological Boos scoring was used to quantitatively assess the IVD degenerative status. Our data indicate that the culture duration tended to increase the modified Boos' score of cultured and non-injected IVDs from a score of 6 at

day 0 to a score of 10 at day 7 (**Fig. 3C**). The Boos' score then remained stable until day 21. A similar trend was observed with cultured, injected IVDs, for which the Boos score was higher immediately following injection (a score of 10 at day 0) and then remained stable until day 21. It is worth noting that the modified Boos score used in this study takes into account the NP cell density, the number of NP tears and granular changes, as well as the presence of NP mucosal degeneration. It ranges from 0 (no IVD degeneration) to 18 (complete IVD degeneration), and the values obtained here hence indicate that the ex vivo culture of IVDs and injection of PMBs did not induce major degenerative processes. In addition, disc cell metabolic activity was assessed on disc sections with an LDH/EtH assay. At each time point, more than 80% of the disc cells were metabolically active, whether or not the IVDs had been injected with PMBs (**Fig. 3D**).

Cell migration in a spontaneously degenerated ovine IVD microenvironment

After having validated our ability to culture an ex vivo organ model of ovine IVD, we were interested in determining whether intradiscally injected PMBs loaded with CCL5 and growth factors can contribute to mobilization, recruitment, and stimulation of stem/progenitors cells (modelized by human ASCs placed on top of the CEP) in our organ culture model. To assess the effect of CCL5/PMBs on cell migration, Vybrant™ DiI-labelled fluorescent human ASCs were seeded on the top cartilaginous endplate of degenerated ovine IVDs (Pfirrmann grade 2-3, as assessed on spine MRIs (**Fig. S1**)) and then tracked for up to 28 days of culture. The experimental design is presented in **Figure 4**, with four conditions: intact IVDs (n=9), IVDs injected with CCL5/PMBs, TGF-β1/PMBs, and GDF-5/PMBs (n=9), IVDs seeded with human ASCs (n=9), and IVDs seeded with human ASCs and then injected with CCL5/PMBs, TGF-β1/PMBs, and GDF-5/PMBs (n=9).

At day 3, 7, and 28, no fluorescent cells were observed in the IVD sections under intact and injected PMB conditions without any seeded hASCs (**Fig. 5A, top row**). By contrast, numerous red-fluorescent cells were observed on sections of IVDs seeded with hASCs, whether or not injected with PMBs (hASCs and hASCs + PMBs groups), at each time point (**Fig. 5A**). The number of fluorescent cells in the NP was determined using ImageJ software, and the results are expressed as the total number of cells that had migrated per section (**Fig. 5B**). While a tendency for an increase in the number of cells per section that had migrated as a function of time was noted for both the seeded hASCs condition (mean values of 11, 12, and 8 at days 3, 7, and 28, respectively) and the seeded hASCs + loaded PMBs condition (mean values of 9, 22, and 12 at days 3, 7, and 28, respectively), there was no significant difference between the groups at the same time point. The maximum migration distance from the endplate to the NP, highlighted by yellow dotted arrows in **Fig. 5A**, was measured and the results are presented in **Fig. 5C** as the mean value of three measurements for each donor (D, E, and G). While the human ASCs migrated a distance of 3-4 mm at day 3 and day 7, respectively, whether or not loaded PMBs where injected, a significant increase in the maximum migration distance was observed at day 28 in the loaded PMBs condition compared to the seeded hASCs condition (7.48 ± 0.42 mm vs. 2.67 mm ± 0.66 mm for donor D, 4.78 mm ± 0.13 mm vs. 5.87 mm ± 0.20 mm for donor E, and 5.07 mm ± 0.41 mm vs. 2.02 mm ± 0.38 mm for donor G, respectively). These data demonstrate that the loaded PMBs did not significantly impact the number of cells that had migrated, although they did significantly increase their migration distance within the disc tissue.

Extracellular matrix histological analysis of ex vivo IVDs

To evaluate the anabolic effects of the seeded human ASCs and the injected loaded PMBs on the NP extracellular matrix, histological Alcian blue (AB), HES, and Masson's trichrome staining were performed on sections at all levels of each condition and at each time point (day 3, day 7, and day 28). Representative coronal sections show the 3 anatomical IVD regions of the IVD (CEPs on the top and bottom, the NP in the centre surrounded by the AF) (**Fig. 6**). While the Alcian blue intensity decreased over time in the intact group (**Fig. 6A**), a slightly more intense blue staining was observed at day 7 and day 28 in all of the experimental groups (hASCs, loaded PMBs, and hASCs + loaded PMBs conditions), particularly in the hASCs + loaded-PMBs group, thus suggesting the formation of an ECM with a higher GAG content. The injected PMBs, composed of a negatively charged polysaccharide network, were identified as blue dots within the NP tissue at each time point, thus indicating that the PMBs withstood the hostile microenvironment of the degenerated IVD throughout the ex vivo culture process (**Fig. 6B**, day 28). No blue dots of this nature were observed in the sections from the groups that were not injected with PMBs, at any time point. It is worth noting that in the hASCs + PMBs condition, the injected PMBs appear to be surrounded by a certain amount of loose blue-stained tissue at day 7 (data not shown) and day 28 (**Fig. 6B**). Regarding the NP cellularity, a quantitative analysis of the HES-stained NP sections of the group seeded with hASCs and injected with PMBs revealed a significant increase of NP cellularity from 36±14 cells per section at day 7 to 100±11 cells per section at day 28 (**Fig. S2**). Moreover, analysis of all groups revealed a signficantly higher cell density at day 28 for the groups seeded with hASCs and injected with PMBs (100±11 cells per section), compared to the NP sections of the groups that were seeded with hASCs and not injected (39±16 cells per section), or not seeded with hASCs (intact (27±1 cells per section) and PMBs (52±25 cells per section) conditions) (**Fig. S2**).

Collagen and aggrecan expression in ex vivo IVDs

Immunostaining of ECM molecules was performed on cryosections at several levels for each condition, and at each time point (day 3, day 7, and day 28). Intense collagen type I immunohistostaining was observed in the vertebral bodies and the AF areas of the IVD sections of all of the groups and at each time point (not shown). Collagen type II was observed throughout the IVD sections, mainly as diffuse matrix staining, for all conditions and at each time point, with a slight increase in the staining intensity at day 28 for the groups seeded with hASCs, whether or not injected with PMBs, compared to the NP sections of the groups that were not seeded with hASCs (intact and PMBs conditions) (**Fig. 7,** top row). On high-magnification images, cytoplasmic expression of type II collagen was observed in cells of the transitional zone (TZ) between the CEPs and the NP, as well as in cells of the NP area (**Fig. 7,** 2nd and 3rd rows). Similarly, diffuse aggrecan staining was observed for all conditions and at each time point, with a slight increase in the staining intensity at day 28 for the groups seeded with hASCs, whether or not injected with PMBs, compared to the NP sections of the groups that were not seeded with hASCs (intact and PMBs conditions)(**Fig. 7,** bottom row). In addition, intracellular staining was observed for all of the groups, except for the intact group, with aggrecan-positive cells mainly localized in the TZ area (not shown), while some aggrecan-positive cells were also observed in the NP.

Tie2-positive cells in ex vivo IVDs

To further analyse the presence and localization of progenitor cells in the ex vivo IVDs, immunohistostaining for a progenitor cell marker, the angiopoietin-1 receptor (Tie2), was carried out. Surprisingly, numerous Tie2-positive cells were observed in all of the spontaneously degenerated IVD sections, for all of the groups and all of the time points (**Fig.8**). After 3 days of ex vivo culture, Tie2-positive cells were found in both the TZ and the NP areas. In the groups that were not seeded with hASCs (intact and PMBs conditions), we observed a rapid decrease in the density of Tie2-positive cells with the ex vivo culture time, with 27±4 and 18±2 cells per section, respectively, at day 3, and only very few positive cells in the NP at day 7 (13±2 and 15±1 cells per section, respectively) and day 28 (11±4 and 8±3 cells per section, respectively). For the group seeded with hASCs but not injected with PMBs, a moderate decrease overtime was also noted, with Tie2-positive cells identified in both the TZ and the NP areas after 3 days (39±25 cells per section), 7 days (25±9 cells per section) and 28 days (18±5 cells per section) of ex vivo culture. By contrast, in the group seeded with hASCs and then injected with loaded PMBs, a significantly higher number of Tie2-positive cells was detected at day 7, compared to all other groups, and at day 28, compared to groups that were not seeded with hASCs (intact and PMBs conditions)(**Fig.S3**).

DISCUSSION

The present work is aimed at development of an injectable sequential release system of chemokine and growth factors in order to stimulate endogenous repair in degenerated IVD. The sequential release steps are essential to i) recruit endogenous stem/progenitor cells to the degenerated NP, and then ii) locally stimulate these cells that have migrated in order to synthesize a healthy extracellular matrix that is rich in aggrecan and type II collagen.

Endogenous disc stem/progenitor cells have recently been discovered and characterized, thereby paving the way to new regenerative strategies while also overcoming many of the difficulties that are often associated with cell therapy. Indeed, cell leakage and death following injection into the NP, as well as osteophyte formation, are partly due to the fact that the injected cells fail to thrive in the disc microenvironment [13,21,23,62]. By contrast, disc stem/progenitor cells have been identified in all three IVD compartments (the CEP, NP, and AF), as well as in vertebral bodies [28,37,63]. Migration routes within the IVD, more precisely pathways connecting the cartilaginous endplates to the centre of the NP, have been hypothesized and subsequently studied [64,65]. Disc stem/progenitor cells exhibit phenotypic similarities and higher osteogenic and chondrogenic differentiation capabilities than bone marrow-derived mesenchymal stem cells (BM-MSCs) [24,26]. Interestingly, disc stem/progenitor cells originating from the CEP have enhanced migratory capacities and they result in a greater degree of chondrogenic regeneration [29,66,67]. As such, the recruitment of disc stem/progenitor cells from the CEPs to the NP appears to be a highly promising endogenous repair strategy.

Understanding the mechanisms of IVD degeneration as well as the failure of repair processes could be the key to designing an effective disc regeneration strategy. Indeed, IVD spontaneous endogenous repair may not be as effective as expected in regard to preventing degeneration [10]. All three major events in IVD degeneration, i.e., inflammation and catabolic cascades, a progressive loss of cells, and a decline in cellular functions and anabolic activities, should be considered for implementation of a robust and sequential repair strategy [68]. Therapeutic strategies should hence address these three events, with the aim of decreasing the catabolic and inflammatory activities in order to make the degenerated IVD microenvironment less hostile, repopulate the partially healed NP tissue, and finally to restore the anabolic activities, and all this by a single intradiscal injection [11,12,47]. However, a chemokine/growth factor delivery approach may still be sufficient to counteract moderate inflammation, notably with TGF-β contributing to maintain the expression level of connective tissue growth factor (CCN2), which decreases the upregulation of MMPs and ADAMTS by inhibition of IL-1β [69–71]. This present work is, therefore, based on a two-step sequential strategy that could take place in a moderately degenerated IVD with restrained inflammatory, catabolic activities, and available disc stem/progenitor cells, which have been reported to decrease with age [30,72].

To develop such a two-step sequential strategy, in the present study we selected the chemokine CCL5 to recruit disc stem/progenitor cells from the periphery of the IVD to the NP, and the growth factors TGF-β1 and GDF-5 to orientate and stimulate the migrated disc stem/progenitor cells to synthesize a nucleopulpogenic ECM. In order to be able to perform a single injection treatment, we combined these factors with pullulan microbeads (PMBs). We

hypothesized that these loaded PMBs would provide appropriate chemokine/growth factor release and biological properties. We analysed the adsorption and release profiles of chemokine CCL5 from PMBs, using the same initial concentrations (1, 2, and 4 µg/mL) as those used in our previous study with growth factors (TGF-β1 and GDF-5) and PMBs [49]. We demonstrated an adsorption efficiency of 100% and a sustained release profile for CCL5, with 99% being released at 21 days with an initial loading concentration of 4 µg/mL. We hypothesized that in this two-step sequential strategy, the released chemokine CCL5 would first recruit disc stem/progenitor cells from the periphery of the IVD to the NP, thus increasing the cell density in the IVD microenvironment, then afterwards the released growth factors TGF-β1 and GDF-5 would stimulate the migrated disc stem/progenitor cells to synthesize an NP-like ECM. Although fast release of CCL5 fits the required profile for cell recruitment in step 1, the previously reported rate of growth factor release (27% for TGF-β1 and 100% for GDF-5) [49] may be too fast to achieve the production of an ECM with appropriate biomechanical properties. Whether such a drug delivery system may allow migrated progenitors to fully differentiate into the nucleopulpogenic pathway remains of particular interest and warrants further analysis. The association of microparticles or microbeads with a macro-hydrogel could slow down the release of biological factors and potentially result in an ideal sequential release profile [68]. This delayed effect has, in fact, been reported for TGF-β1/PMBs and GDF-5/PMBs dispersed in a cellulose-based hydrogel [49]. A polymer of choice could be hyaluronic acid, which is one of the main components of the NP ECM and which has been used as a thermoreversible hydrogel to deliver another chemokine, CXCL12 (Chemokine (CXC) ligand factor 12, also called stromal cell-derived factor-1, or SDF-1 [54–56]. In this study, a burst release of SDF-1 (~27%) was observed within the first 6 h, after which the release continued slowly, reaching about 54% after 7 days. The maximum release of SDF-1 was observed at 24 h, and a significant increase of the number of cells migrating into nucleotomized discs compared with discs treated with a solution of SDF-1 was observed at 48 hours. In order to extend the duration of the release, complex delivery systems might be necessary. IVD-specific approaches for local and sustained delivery of fragile biologics into IVDs were recently reviewed, including multiscale combined systems associating in situ-forming hydrogels with ready-to-use micro- or nano- particles [12].

Regarding the CCL5 chemoattractant activity, the trend of enhanced cell migration overtime obtained with CCL5/PMBs compared to unloaded PMBs and free chemokines confirmed that the protection provided by the biomaterial is a fundamental aspect to ensure a sustained biological effect. This is in line with the retention of the biological activity of TGF-β1 and GDF-5 after their release from PMBs, i.e., the ability to phosphorylate components of the SMAD (2/3 and 1/5/8) pathways of hASCs, that was demonstrated previously [49]. As reported in the literature, we found -as expected- that the chemotaxis results varied substantially between donors. This is in agreement with a study that, by assessing the effect of the donor's age on cell migration, found that human BM-MSCs isolated from young donors exhibited a significantly higher migration capacity in a bovine ex vivo model compared to cells from older donors [54]. To overcome this variability, we increased the number of in vitro experiments with different donors and we confirmed that a significant increase in migration was achieved with released CCL5 for three out of four human donors, with similar profiles obtained for all of the human donors.

Ex vivo IVD culture organ models have recently been developed by several research teams in order to evaluate disc stem/progenitor cell migration routes. We first validated our culture conditions, based on protocols developed by the AO Foundation [61], using lumbar IVDs isolated from young sheep. Our histological and cell metabolism data collectively show that we have, for the first time, successfully implemented an ex vivo culture model of lumbar ovine IVD for at least 3 weeks and that it can be used to monitor the effects of intradiscally injected biologics. We then implemented a degenerative model to study the chemoattractant potential of our sequential release system. Previous studies were performed in caudal IVDs that were isolated from calves and then submitted to a nucleotomy to degenerate the initially healthy tissue [61]. However, this induced microenvironment to mimic a degenerative tissue is not representative of a naturally damaged IVD. We, therefore, wished to use a spontaneously degenerated microenvironment. We hence selected sheep IVDs, which are known to undergo spontaneous IVD degeneration with age, as a more relevant animal model [73,74]. Testing of CCL5/PMBs, TGF-β1/PMBs, and GDF-5/PMBs was then performed with this age-dependent spontaneous degenerative model using lumbar IVDs harvested from 3- to 7-year-old sheep. While spontaneous disc degeneration models are highly clinically relevant, they also suffer from several drawbacks compared to induced degeneration models. In addition to the inherent inter-discal variability within a given animal, this is an uncontrolled and less repeatable model due primarily to the significant inter-donor variability of the disc degeneration. In addition, the model has turned out to be technically challenging, with the presence of osteophytes that hampers cryosectioning of the decalcified samples. Nonetheless, this spontaneous model of IVD degeneration in a large animal model is a considerable asset for performing an ex vivo proof of concept of a novel therapeutic approach. To our knowledge, this is the first study to report an ex vivo model of naturally degenerated IVD.

Using this ex vivo spontaneously degenerated IVD model, we were able to document an increasing trend in terms of the number of migrated hASCs and a significant increase in the hASCs migration distance when we used the CCL5/TGF-β1/GDF-5 PMBs sequential release system. We were also able to show that there was spontaneous cell migration, in agreement with what has been reported in ex vivo caudal bovine IVDs, and this was probably due to chemokines secreted by the degenerated disc cells, notably CCL5 [32,33]. Another study performed in an ex vivo nucleotomized bovine IVD showed that, while injected soluble SDF-1 had no chemoattractant activity, suggesting that the soluble protein might be prone to degradation in the tissue, hyaluronan-poly(N-isopropylacrylamide) (HAP) hydrogels exhibited maximal release of SDF-1 at 24 h. In addition, there was a significant increase in the proportion of human BM-MSCs that had migrated from the CEP toward the NP after 48 hours [54]. It is worth noting that several ex vivo studies have been performed using bioreactors whereby the IVD tissues were submitted to high-frequency loading (10 Hz) to induce degeneration [32,33]. In these conditions, secretion of CCL5 by the degenerated disc cells was enhanced and resulted in a chemotactic effect on human MSCs. Since we used sheep IVDs that exhibited age-related degeneration, implementation of a bioreactor using “physiological loading” at low frequency (0.2 Hz) could be performed to investigate cell recruitment.

The progenitor cell marker Tie2 has already been described in the mouse, canine, bovine, and human NP [30,75,76]. These studies demonstrated that, unlike Tie2-negative cells, Tie2-positive cells isolated from NP tissue

could differentiate into the mesenchymal lineage [75]. For the first time, we report the presence of Tie2-positive cells in ovine IVDs. The rapid loss of Tie2-positive cells in ovine degenerated IVDs that were cultured for 7 days or 28 days (intact groups) is in accordance with the reported decrease with age and degeneration of Tie2 progenitor cells in the murine and human NP [30]. Interestingly, increased NP cellularity was observed in the condition where hASCs were seeded on the top endplate compared to the control group. While both healthy and herniated human IVDs have been reported to exhibit a low level of cell proliferation [77,78], stimulation of NP cell proliferation has been described when IVDs are injured by nucleotomy. Moreover, the injection of loaded PMBs resulted in preservation of Tie2-positive cells in the NP tissue overtime compared to day 0. These results suggest that the combination of CCL5/TGF-β1/GDF-5 PMBs could have either enhanced the migration of hASCs from the CEP toward the NP, stimulated the migration of endogenous progenitor cells from the CEP toward the NP, or enhanced expression of the Tie2 marker in resident NP cells. Interestingly, it has been reported that hASCs promote expression of the Tie2 marker by progenitor cells [79,80]. Human anti-mitochondrial immunolabelling has not been successful, and we are currently investigating another way to label human cells in order to confirm these hypotheses.

In this study, we selected hASCs as substitute for IVD stem/progenitor cells, as well as for their demonstrated ability to differentiate into NP-like cells when cultured in the presence of TGF-β1 and GDF-5 [46]. We speculate that hASCs that migrated from the CEP were able to attenuate IVD degeneration through ECM remodelling and the synthesis of a healthy NP ECM. As such, increasing the recruitment of disc stem/progenitor cells to a degenerated NP could increase ECM remodelling, thereby enhancing the tissue regenerative potential. In vivo, CCL5 could also mediate the recruitment of immune cells, which would then propagate inflammation and amplifiy tissue damage [81,82]. It will be interesting to explore the mechanisms by which cells invade the IVD tissue. It has been hypothesized that ECM degradation by MMPs secreted by degenerative cells plays a role, and upregulation of MMP13 and MMP7 has been demonstrated in an ex vivo bovine IVD model cultured under degenerative conditions [32].

The next step of the study will be to perform an in vivo proof of concept in sheep with degenerated IVDs exhibiting Pfirrmann scores between 2 and 3, in order to confirm the regenerative potential of this chemokine/growth factor sequential delivery system. The intradiscal injectability in delicate and hard-to-reach IVD tissue should be considered. Injectability by means of a 23G needle has been demonstrated for PMBs alone and PMBs dispersed within a macro-hydrogel [49]. Trans-annular injection is the most commonly studied method and it is being used in ongoing clinical studies. It is worth noting that the transpedicular approach has recently been described as an alternative route, but long-term effects on the endplate integrity have not yet been evaluated and signs of a degree of induced degeneration have been reported [83].

CONCLUSION

This study demonstrates that pullulan microbeads (PMBs) constitute a suitable microcarrier for CCL5 chemokine and TGF-β1 / GDF-5 growth factors, thereby allowing their sequential and sustained release and maintenance of their biological activity, i.e., the in vitro ability to enhance cell migration, as well as the ability to activate SMAD signalling [49]. We also demonstrated that this sequential release system significantly increased the distance that human ASCs were able to migrate toward the NP, using a newly described ex vivo degenerated ovine IVD model. In addition, the overall NP cellularity, the collagen type II and aggrecan staining intensity, and the Tie2-positive progenitor cell density in the NP were increased at day 28 compared to the control groups. The results presented here constitute a proof of concept that PMBs loaded with CCL5/TGF-β1/GDF-5 constitute an innovative sequential release system for endogenous IVD regeneration.

ACKNOWLEDGMENTS

LF is a recipient of an MESR PhD scholarship. The authors gratefully acknowledge S. Grad (AO foundation, Davos, Switzerland) for her help with implementing the ex vivo ovine model of IVDs. The authors thank Dr F. Lejeune (Clinique Breteche, Nantes) for harvesting the human lipoaspirates. The authors also thank the CRIP (O. Gauthier, N. Boushina, C. Decante, P. Roy, D. Rouleau, S. Madec, and I. Leborgne) for providing the sheep spines and the MicroPICell platform from the SFR Francois Bonamy/INSERM UMS 016 (P. Hulin, S. Nedellec, and P. Paul-Gilloteaux) for the confocal microscopy.

FUNDING SOURCES

This study was supported by grants from the Région des Pays de la Loire (BIO2), ANR (STIMUDISC - ANR-16-CE18-0008 and REMEDIV ANR-14-CE16-0017) and the Fondation de l'Avenir (AP-RMA 2015-018 and BO-RMA-15-001).

DECLARATIONS OF INTERESTS

The authors declare no financial conflicts of interest.

AUTHOR CONTRIBUTIONS

LF, CC, CM, ES, MA, BH, and JL performed experiments. LF collected the data. LF, JC, MF, JG, and CLV designed the study and analysed the data. LF, JG, and CLV drafted, edited and revised the manuscript. All authors reviewed and approved the manuscript.

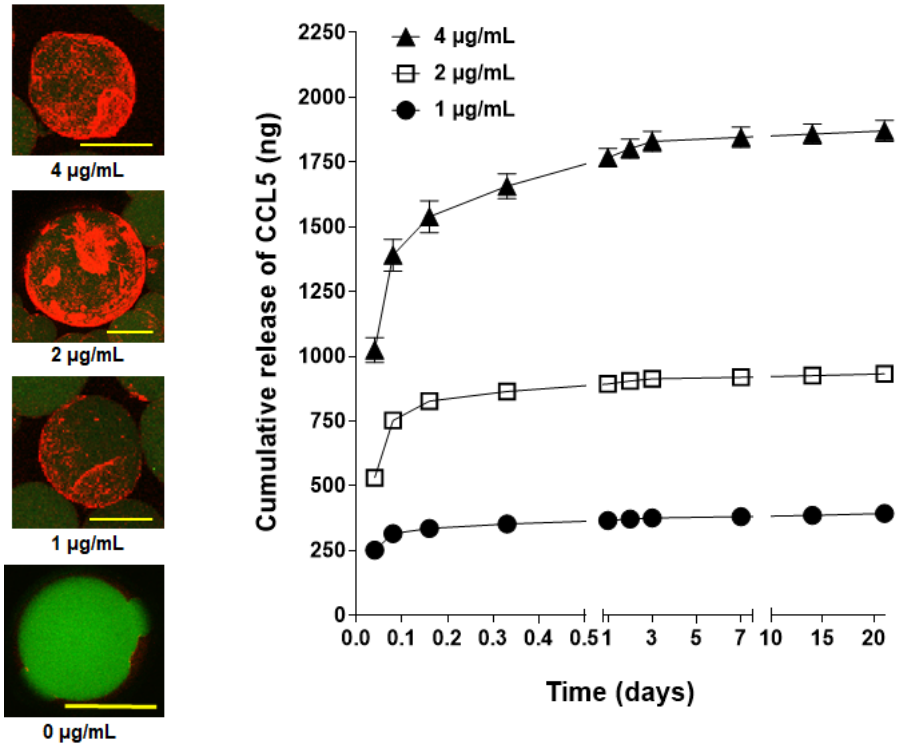

Figure 1. CCL5 chemokine adsorption and release kinetics from pullulan microbeads (PMBs). The PMBs were loaded by incubation with CCL5 (1, 2, or 4 µg/mL in PBS) and stirred at 4 °C for 24 hours. In one experiment, the loaded PMBs were fixed with PFA and immunolabelled with anti-CCL5 antibody, followed by secondary antibodies conjugated to Alexa Fluor® (577 nm) fluorophores. Images of the chemokine on the surface of the PMBs were obtained by confocal fluorescence microscopy (scale bar 100 µm). In another experiment, release of the chemokine from the loaded PMBs took place with stirring in 500 µL of PBS/1% w/v BSA at 37 °C for 21 days. Aliquots of supernatants were retrieved at specific time points and analysed by ELISA for CCL5. The results are expressed as the cumulative amount of released CCL5 as a function of time. The experiments were performed in triplicate and the results are expressed as means ± the SD. Abbreviations: CCL5: chemokine (C-C motif) ligand 5; PFA: paraformaldehyde.

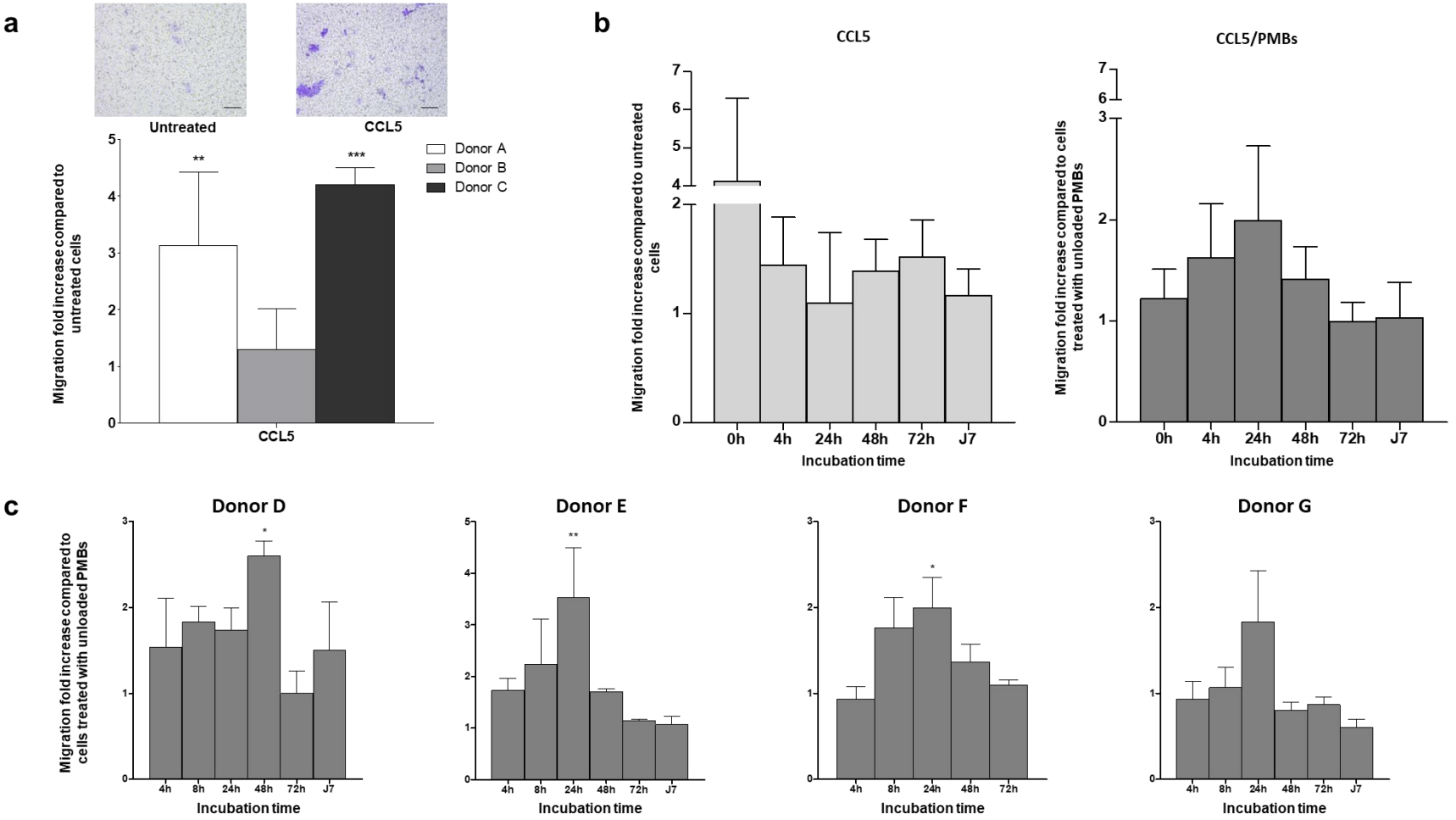

Figure 2. In vitro bioactivity of CCL5 on human ASC migration. (a) Migratory effect of CCL5 on human ASCs. The in vitro migration over a four-hour period of human ASCs treated with CCL5 (250 ng/mL in DMEM/0.1% w/v BSA) and of untreated cells (DMEM/0.1% w/v BSA) are presented. Representative microscopy images of the lower side of the

inserts, with crystal violet staining of the cells that had migrated, are shown (scale bar 100 μm). The results for three donors (donors A, B, and C) were independently expressed as the fold increase compared to their own control groups (untreated cells) and they are presented as means ± the SD of triplicate experiments. (b) Sustained bioactivity of CCL5. The migratory effect of free CCL5 on human ASCs was assessed as a function of time. Free CCL5 (4 μg/mL) in DMEM/0.1% w/v BSA was incubated at 37 °C. At specific time points (fresh solution or suspension, 4 h, 24 h, 48 h, 72 h, and 7 days of incubation), human ASCs were seeded on transwell inserts and a migration assay was then performed for 4 hours, with cells in the presence of the incubated free chemokines. The results are expressed as the fold increase compared to untreated cells at each time point, pooled for all of the donors (donors D, E, F, and G). The untreated cells were incubated with DMEM/0.1% w/v BSA. (c) Sustained bioactivity of CCL5 released from PMBs. The migratory effect of CCL5 released from PMBs on human ASCs was assessed as a function of time. CCL5/PMBs (initial loading concentration 4 μg/mL) in DMEM/0.1% w/v BSA were incubated at 37 °C. At specific time points (fresh solution or suspension, 4 h, 24 h, 48 h, 72 h, and 7 days of incubation), human ASCs were seeded on transwell inserts and a migration assay was then performed for 4 hours, with cells in the presence of the incubated CCL5/PMB. Cells from four donors (D, E, F, and G) were used to assess the bioactivity of the CCL5/PMBs over time. For each time point and donor, the migration results are expressed as the fold increase compared to cells treated with unloaded PMBs at the same time point. The results are presented as means ± the SD for four donors (donors D, E, F, and G), and all of the experiments were performed in triplicate. *represents a significant difference with untreated cells, ** $p < 0.01$, *** $p < 0.001$, two-way ANOVA, Bonferroni post-test. Abbreviations: CCL5: chemokine (C-C motif) ligand 5; ASCs: adipose stem cells; BSA: bovine serum albumin; PMBs: pullulan microbeads.

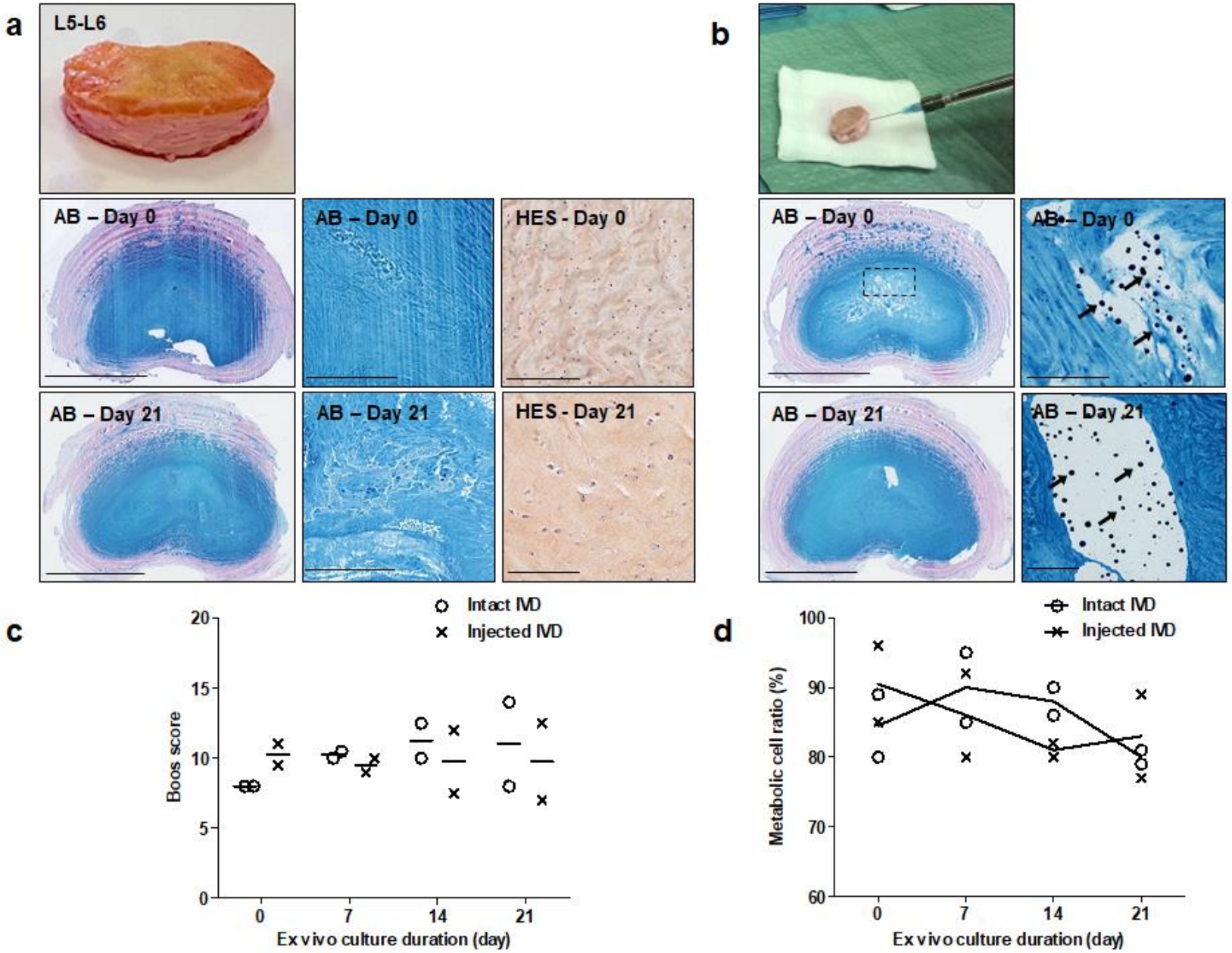
a
L5-L6
AB – Day 0
AB – Day 0
HES - Day 0
AB – Day 21
AB – Day 21
HES - Day 21
b
AB – Day 0
AB – Day 0
AB – Day 21
AB – Day 21
c
Intact IVD
Injected IVD
Boos score
Ex vivo culture duration (day)
d
Intact IVD
Injected IVD
Metabolic cell ratio (%)
Ex vivo culture duration (day)

Figure 3. Long-term ex vivo culture of ovine IVDs. (a) Lumbar IVDs (n=16) were harvested from young sheep, with a spine MRI performed immediately post-mortem (Pfirrmann grade 1). The IVDs were cultured for up to 21 days, cryosectioned, and then histologically stained with Alcian blue (AB) and haematoxylin/eosin/saffron (HES) to analyse the ECM content and cell density over time (scale bar 10 mm for the whole IVD section and 2.5 mm for the high magnification). (b) IVDs (n=8) were injected with unloaded PMBs (0.8% w/w in PBS), cryosectioned, and then histologically stained (scale bar 10 mm for the whole IVD section and 2.5 mm for the high magnification). Injected PMBs observed within the NP tissue at day 0 and day 21 are indicated with black arrows. (c) The Boos score was measured on histologically stained sections of intact (non-injected; n=8, with 2 discs used per time point) and injected IVDs (n=8, with 2 discs used per time point). (d) Cell metabolism in the NP and AF was evaluated with an LDH/EtH assay. The results are expressed as the percentage of metabolically active cells (labelled by LDH) relative to the total number of cells. The experiments were performed on two IVDs per time point for each condition (non-injected and injected). Abbreviations: IVD: intervertebral disc; AB: Alcian blue; HES: haematoxylin eosin saffron; NP: nucleus pulposus; PMBs: pullulan microbeads, LDH: lactate dehydrogenase; EtH: ethidium homodimer.

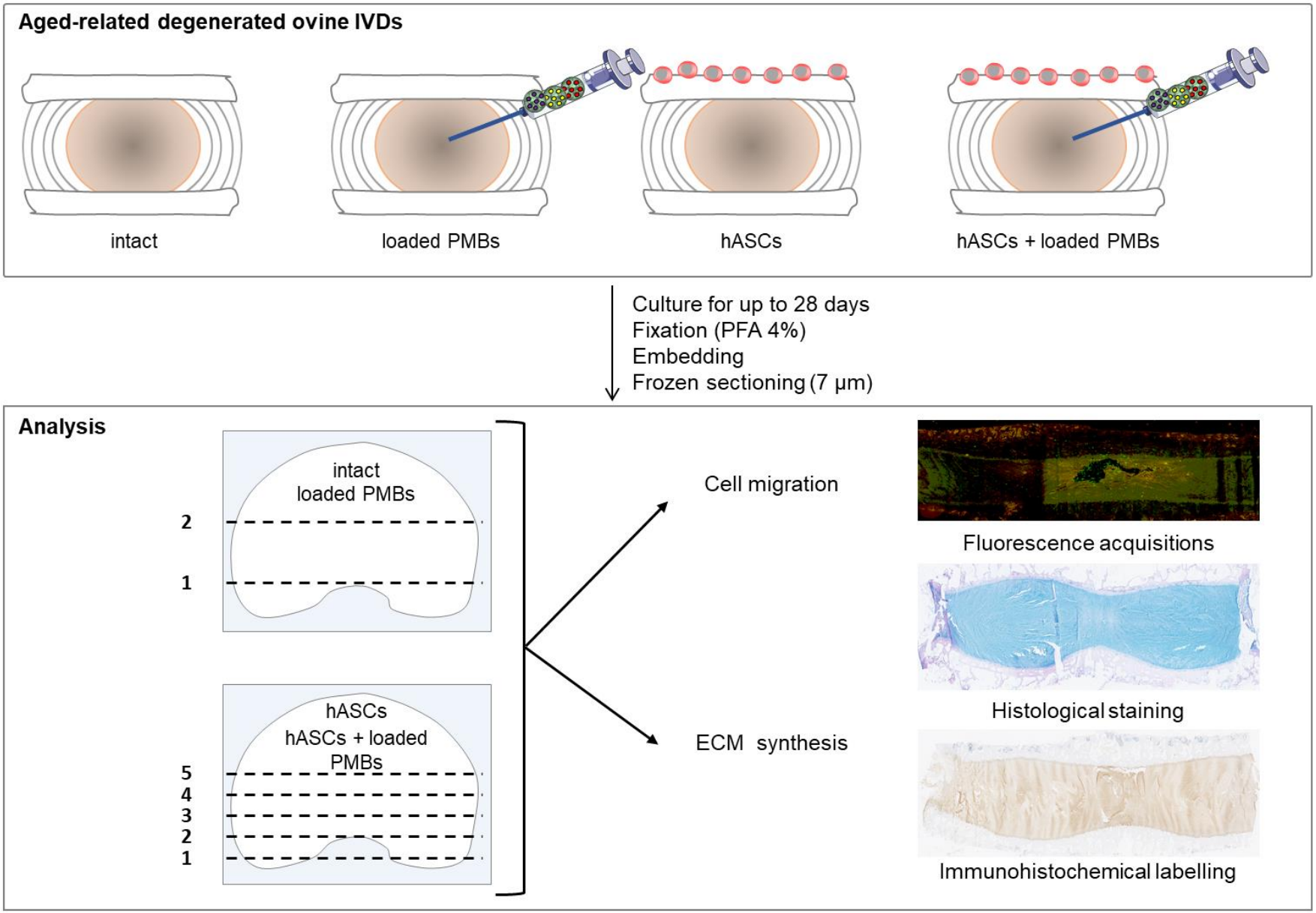
Aged-related degenerated ovine IVDs
intact
loaded PMBs
hASCs
hASCs + loaded PMBs
Culture for up to 28 days
Fixation (PFA 4%)
Embedding
Frozen sectioning (7 µm)
Analysis
intact
loaded PMBs
2
1
hASCs
hASCs + loaded PMBs
5
4
3
2
1
Cell migration
ECM synthesis
Fluorescence acquisitions
Histological staining
Immunohistochemical labelling

Figure 4. Schematic representation of the experimental design for studying cell migration and disc regeneration. An ex vivo organ culture model was performed by using age-related degenerated ovine IVDs. Four conditions were evaluated, with 9 intact IVD controls (intact group), 9 IVDs seeded with Vybrant™ DiI-labelled human ASCs (hASCs group), 9 IVDs injected with CCL5/PMBs, TGF-β1/PMBs, and GDF-5/PMBs (loaded-PMBs group), and 9 IVDs seeded with Vybrant™ DiI-labelled human ASCs and then injected with CCL5/PMBs, TGF-β1/PMBs, and GDF-5/PMBs (hASCs + loaded-PMBs group). At each time point (3, 7, and 28 days of culture), the IVDs were fixed with 4% PFA and then frozen and sectioned coronally (7 µm). The IVDs that were not seeded were cut at 2 levels and the IVDs seeded with cells were cut at 5 levels, with 40 sections per level for all of the IVDs. To evaluate the migration, red-fluorescent cells were observed using a NanoZoomer® slide scanner. For analysis of the ECM, the slides were histologically stained (Alcian blue, haematoxylin/eosin/saffron, and Masson's trichrome) and labelled immunohistochemically (type I collagen, type II collagen, aggrecan, and Tie2). Abbreviations: ASC: adipose stem cells; IVD: intervertebral disc; PMBs: pullulan microbeads; CCL5: chemokine (C-C motif) ligand 5; TGF-β1: transforming growth factor-β1; GDF-5: growth differentiation factor 5; ECM: extracellular matrix; PFA: paraformaldehyde.

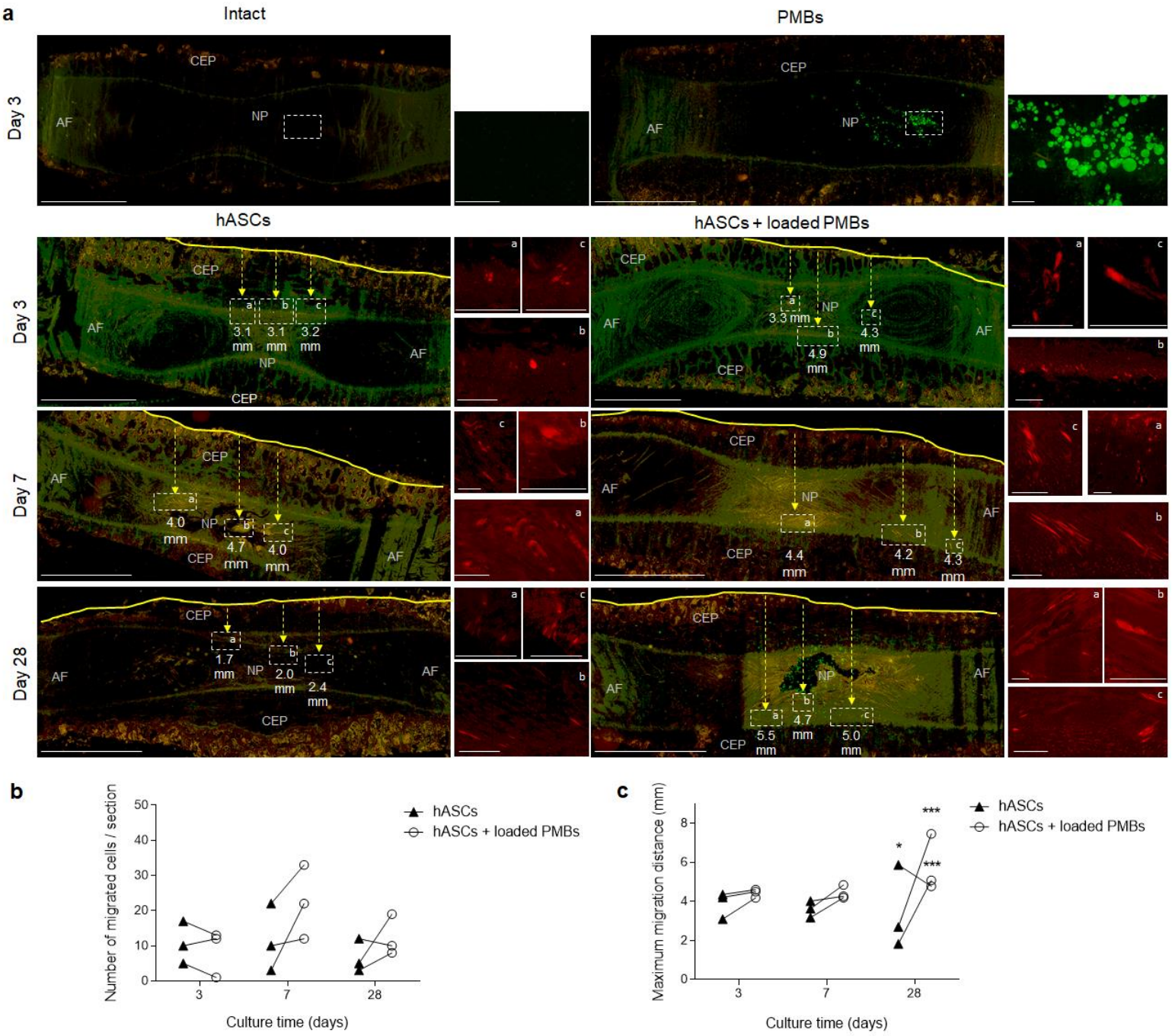
a
Intact
PMBs
hASCs
hASCs + loaded PMBs
Day 3
Day 7
Day 28
CEP
AF
NP
3.1 mm
3.1 mm
3.2 mm
3.3 mm
4.9 mm
4.3 mm
4.0 mm
4.7 mm
4.0 mm
4.4 mm
4.2 mm
4.3 mm
1.7 mm
2.0 mm
2.4 mm
5.5 mm
4.7 mm
5.0 mm
b
Number of migrated cells / section
hASCs
hASCs + loaded PMBs
Culture time (days)
c
Maximum migration distance (mm)
hASCs
hASCs + loaded PMBs
Culture time (days)

Figure 5. Cell migration in spontaneously degenerated ex vivo ovine IVDs. IVDs (n=36) were isolated from 6 sheep (3-7 years old) that exhibited moderate lumbar degeneration (Pfirrmann grade 2 or 3). The top cartilaginous endplates were seeded with human ASCs (n=9 discs, donors D, E, and G), freshly labelled with Vybrant™ DiI, and PMBs loaded with CCL5, TGF-β1, and GDF-5 (0.8% w/w in PBS) were injected via a trans-annular injection into the NP at day 0. Control discs were either only injected with PMBs (n=9 discs), only seeded with human ASCs (n=9 discs), or kept intact (n=9 discs). After 3, 7, or 28 days of culture, the IVDs were fixed with 4% PFA and then frozen and coronally sectioned (7 µm). To evaluate cellular migration, red-fluorescent cells were observed using a NanoZoomer® slide scanner. (a) Representative fluorescent images of IVD frozen sections at 3 and 28 days. The high-magnification inserts highlight the migrated red-fluorescent cells observed at the greatest distance from their seeding point, with dotted arrows indicating the distance covered by the cells (scale bars: low magnification 5 mm, high magnification 250 µm). (b) Cells that had migrated into the NP were identified and counted using ImageJ software. The results are presented as the mean value of the number of cells that had migrated per section, with 5 sections (each separated by 500 µm) analysed per disc and per time point. The values from three donors are represented. (c) The maximum migration distance from the endplate (highlighted with a yellow line) toward the NP was measured using NDP.scan software. For each section, time point, and donor, the results are presented as the mean value of 3 measurements performed on a single section. Abbreviations: ASCs: adipose stem cells; IVD: intervertebral disc; PMBs: pullulan microbeads; CCL5: chemokine (C-C motif) ligand 5; TGF-β1: transforming growth factor-β1; GDF-5: growth differentiation factor 5; ECM: extracellular matrix; PFA: paraformaldehyde.

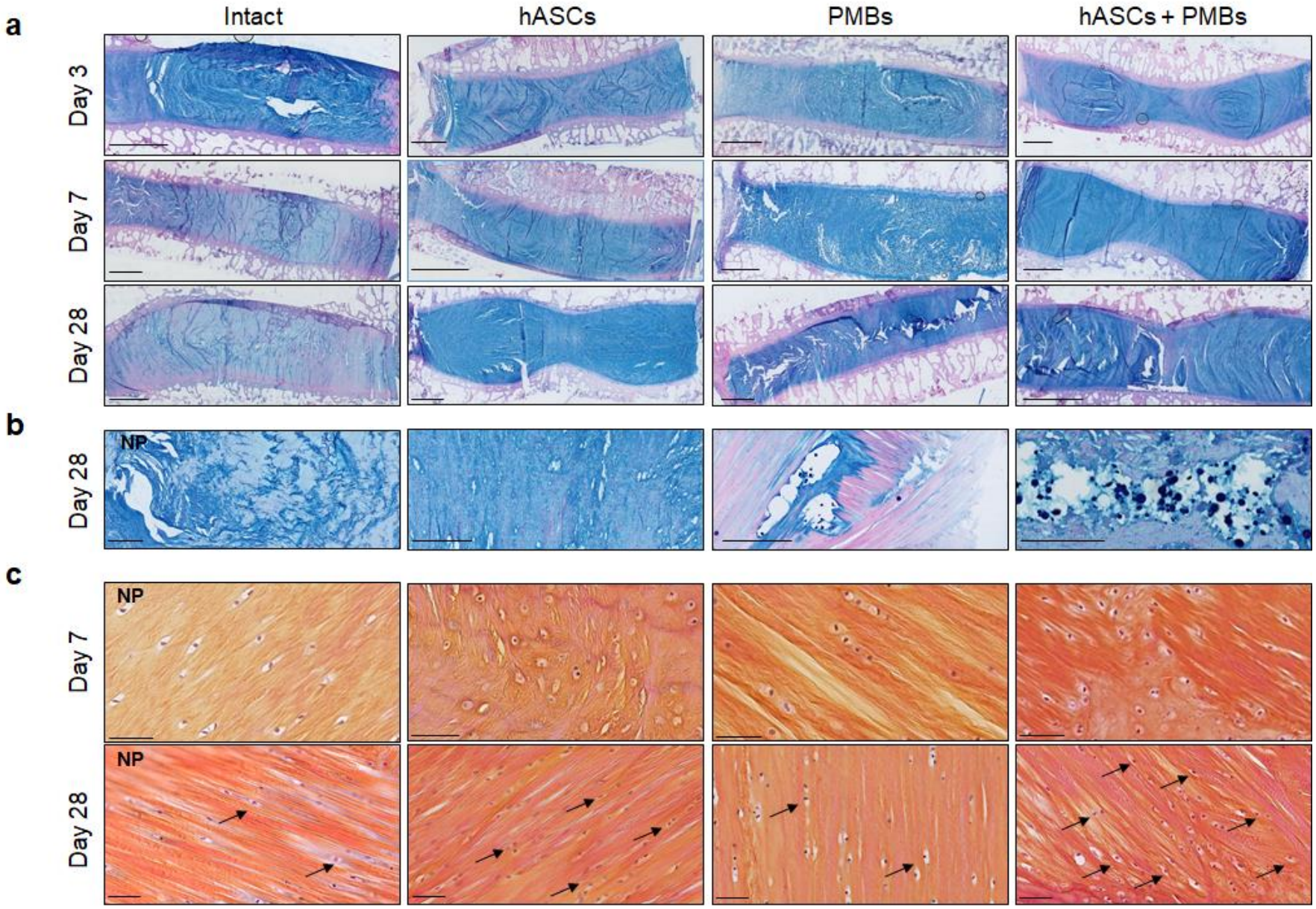
a
Intact
hASCs
PMBs
hASCs + PMBs
Day 3
Day 7
Day 28
b
Day 28
NP
c
Day 7
NP
Day 28
NP

Figure 6. Histological analysis of spontaneously degenerated ex vivo ovine IVDs. Lumbar IVDs (n=36) were harvested from 6 sheep (3-7 years old) that exhibited moderate lumbar degeneration (Pfirrmann grade 2 or 3). The top cartilaginous endplates were seeded with human ASCs (n=9 discs, donors D, E, and G), freshly labelled with Vybrant™ DiI, and PMBs loaded with CCL5, TGF-β1, and GDF-5 (0.8% w/w in PBS) were injected via a trans-annular injection into the NP at day 0. Control discs were either only injected with PMBs (n=9 discs), only seeded with human ASCs (n=9 discs), or kept intact (n=9 discs). Following 3, 7, or 28 days of culture, the IVDs were fixed with 4% PFA, frozen, coronally sectioned (7 µm), and then histologically stained with Alcian blue (AB) and haematoxylin/eosin/saffron (HES) to analyse the ECM content and the cell density, respectively. (a) Representative whole IVD sections stained with AB (scale bar 2.5 mm). (b) High magnification of AB-stained sections with negatively charged PMBs identified as blue dots within the NP tissue at day 28 (scale bar: 500 µm). (c) High magnification of HES-stained sections, with cells labelled with black arrows (scale bar 50 µm). Abbreviations: IVD: intervertebral disc; ASCs: adipose stem cells; PMBs: pullulan microbeads; CCL5: chemokine (C-C motif) ligand 5; TGF-β1: transforming growth factor-β1; GDF-5: growth differentiation factor 5; NP: nucleus pulposus; PFA: paraformaldehyde; AB: Alcian blue; HES: haematoxylin eosin saffron; ECM: extracellular matrix.

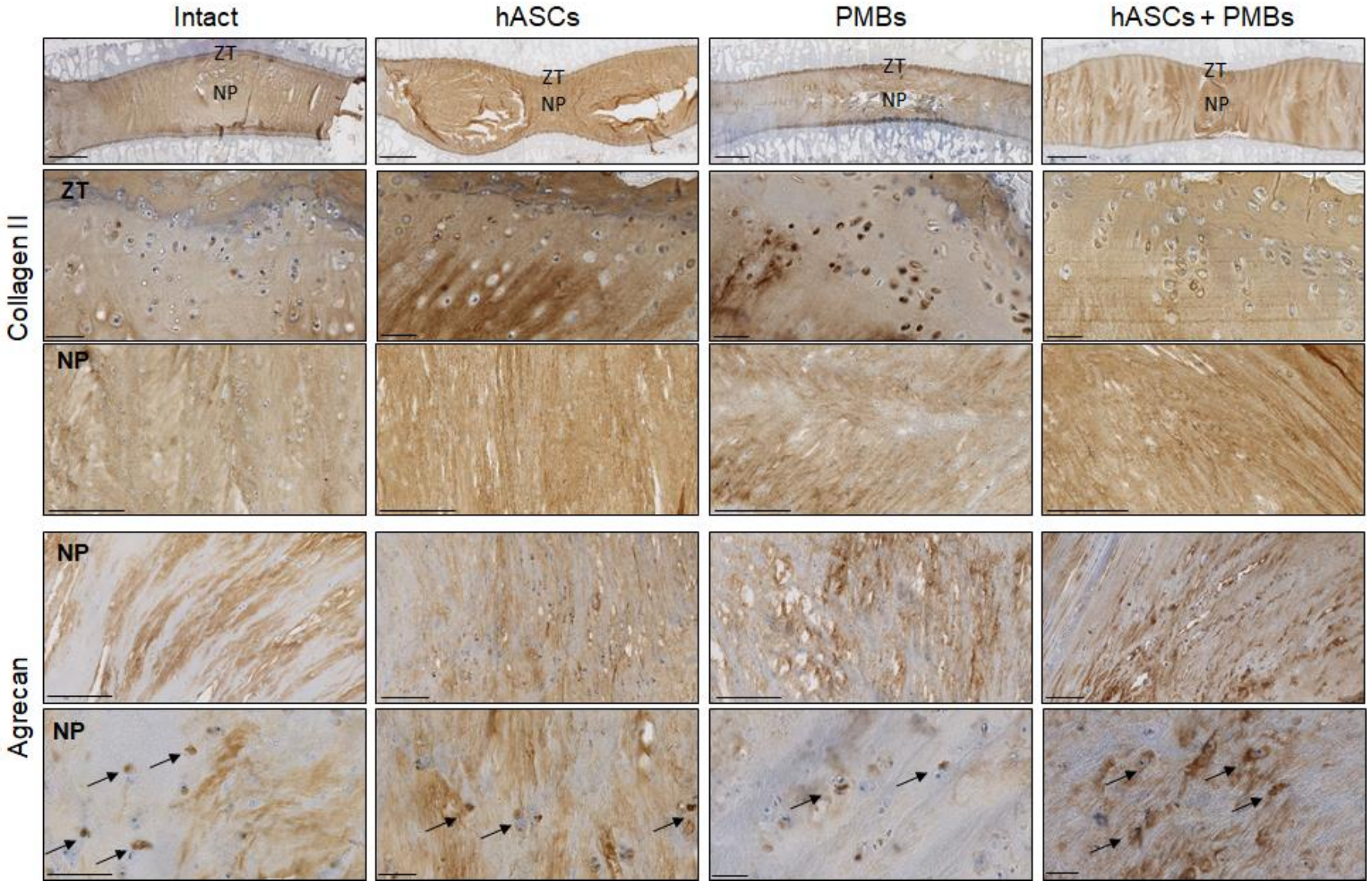
Intact
hASCs
PMBs
hASCs + PMBs
ZT
NP
Collagen II
Agrecan

Figure 7. Collagen and aggrecan immunostaining in age-related degenerated ex vivo ovine IVDs. Lumbar IVDs (n=36) were harvested from 6 sheep (3-7 years old) that exhibited moderate lumbar degeneration (Pfirrmann grade 2 or 3). The top cartilaginous endplates were seeded with human ASCs (n=9 discs, donors D, E, and G), freshly labelled with Vybrant™ DiI, and PMBs loaded with CCL5, TGF-β1, and GDF-5 (0.8% w/w in PBS) were injected via a trans-annular injection into the NP at day 0. Control discs were either only injected with PMBs (n=9 discs), only seeded with human ASCs (n=9 discs), or kept intact (n=9 discs). After 3, 7, or 28 days of culture, the IVDs were fixed with 4% PFA, cryosectioned coronally (7 µm), and then immunohistologically labelled with type II collagen and aggrecan antibodies. Representative whole IVD sections (day 28) immunolabelled for type II collagen (top row, scale bar 2.5 mm), with high magnifications of TZ (scale bar 50 µm) and NP regions (scale bar 250 µm). Representative low-magnification (top row, scale bar 250 µm) and high-magnification NP sections (scale bar 50 µm) (day 28) immunolabelled for aggrecan. Abbreviations: IVD: intervertebral disc; ASCs: adipose stem cells; PMBs: pullulan microbeads; NP: nucleus pulposus; TZ: transitional zone; PFA: paraformaldehyde; ECM: extracellular matrix.

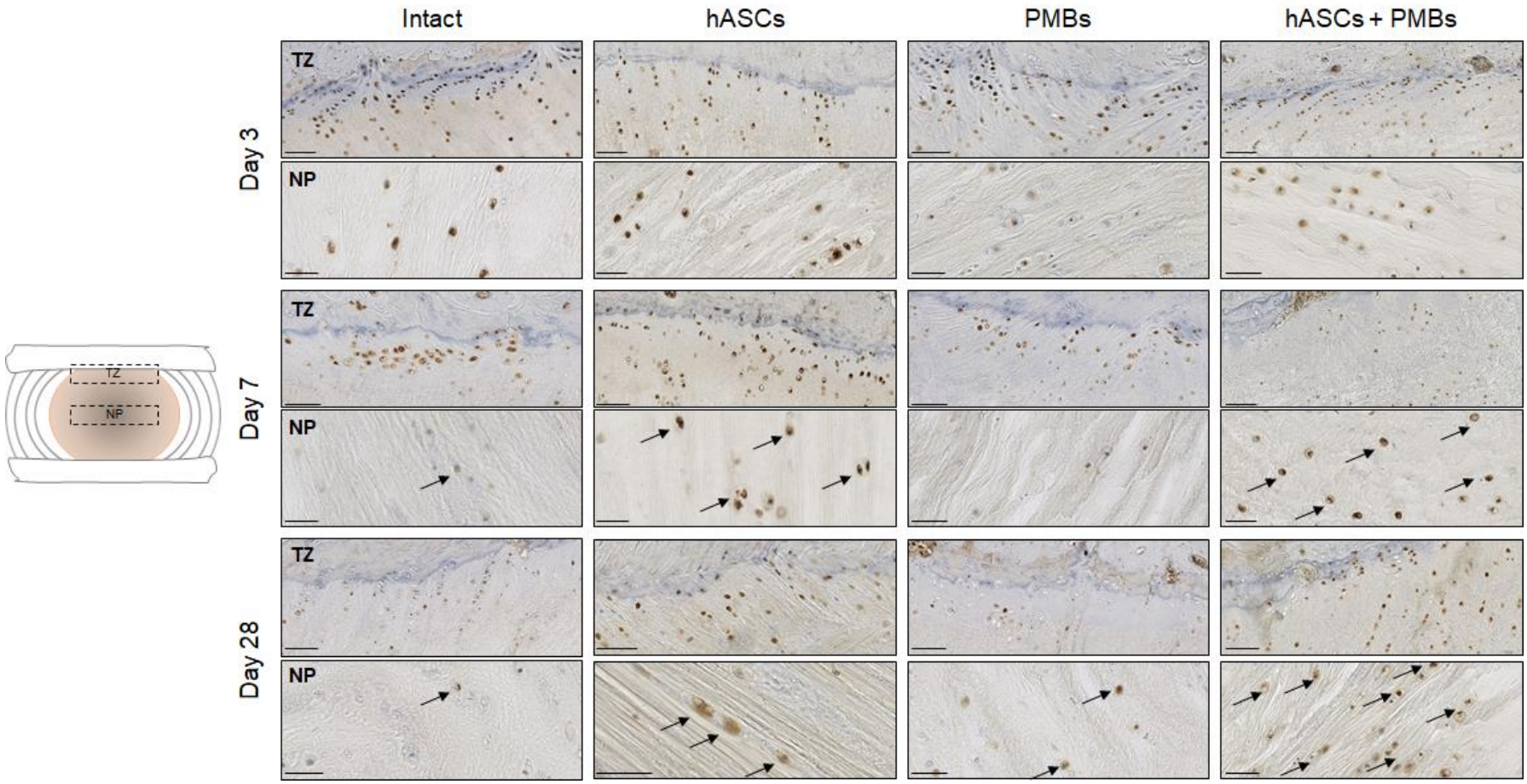

Figure 8. Tie2+ cell immunostaining in age-related degenerated ex vivo ovine IVDs. Lumbar IVDs (n=36) were harvested from 6 sheep (3-7 years old) that exhibited moderate lumbar degeneration (Pfirrmann grade 2 or 3). The top cartilaginous endplates were seeded with human ASCs (n=9 discs, donors D, E, and G), freshly labelled with Vybrant™ DiI, and PMBs loaded with CCL5, TGF-β1, and GDF-5 (0.8% w/w in PBS) were injected via a trans-annular injection into the NP at day 0. Control discs were either only injected with PMBs (n=9 discs), only seeded with human ASCs (n=9 discs), or kept intact (n=9 discs). After 3, 7, or 28 days of culture, the IVDs were fixed with 4% PFA, cryosectioned coronally (7 µm), and then labelled immunohistologically with Tie2 antibodies. Representative images of the transitional zone between the CEPs and the NP (TZ, scale bar 100

μm) and the central NP region (NP, scale bar 50 μm) within the same IVD section, for each group at day 3, 7, and 28. Abbreviations: IVD: intervertebral disc; ASCs: adipose stem cells; PMBs: pullulan microbeads; TZ: transitional zone; NP: nucleus pulposus; PFA: paraformaldehyde; ECM: extracellular matrix.

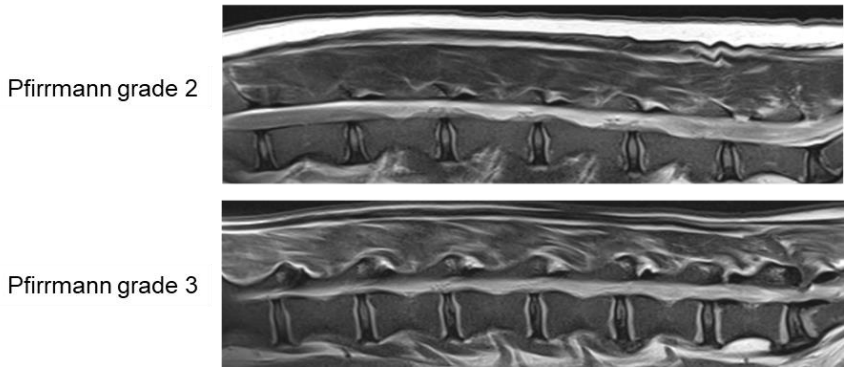

Figure S1. Representative MRIs of the ovine spines used for the spontaneous IVD degeneration ex vivo model.

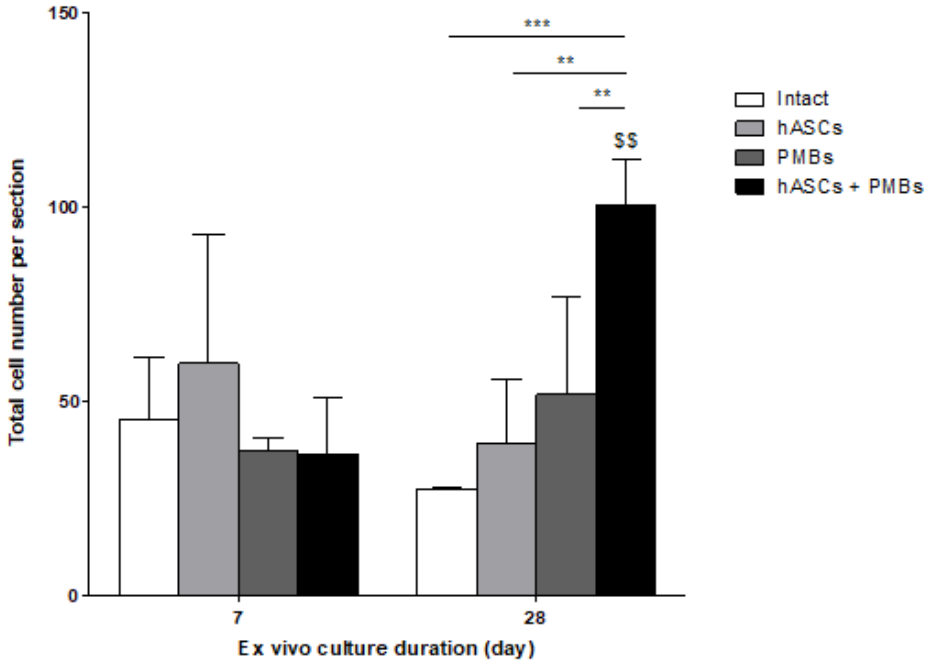

Figure S2: Quantification of cellularity in aged-related degenerated ex vivo ovine IVDs. IVDs (n=36) were isolated from 6 sheep (3-7 years old) presenting moderate lumbar degeneration (Pfirrmann's grade 2 or 3). Top cartilaginous endplates were seeded with human ASCs (n=9 discs, donors D, E and G), freshly labeled with VybrantTM DiI, and loaded PMBs with CCL5, TGF-β1 and GDF-5 (0.8 % w/w in PBS) were injected via a trans-annular injection in the NP at day 0. Control discs were either only injected with PMBs (n=9 discs), only seeded with human ASCs (n=9 discs), or 9 others kept intact (n=9 discs). After 7 or 28 days of culture, IVDs were fixed with PFA 4% then coronally frozen sectioned (7 µm). Cells in the central NP region were identified on high magnification HES stained sections and counted using NDP view software. For each section, time point and donor, results are presented as the mean value of 5 measurements performed on one section. * represents a significant difference between groups, ** $p<0.01$, *** $p<0.001$, two way ANOVA, Bonferroni post-test. $ represents a significant difference between day 7 and day 28, $$ $p<0.01$. Abbreviations: IVD: intervertebral disc; ASCs: adipose stem cells; PMBs: pullulan microbeads; NP: nucleus pulposus; PFA: paraformaldehyde.

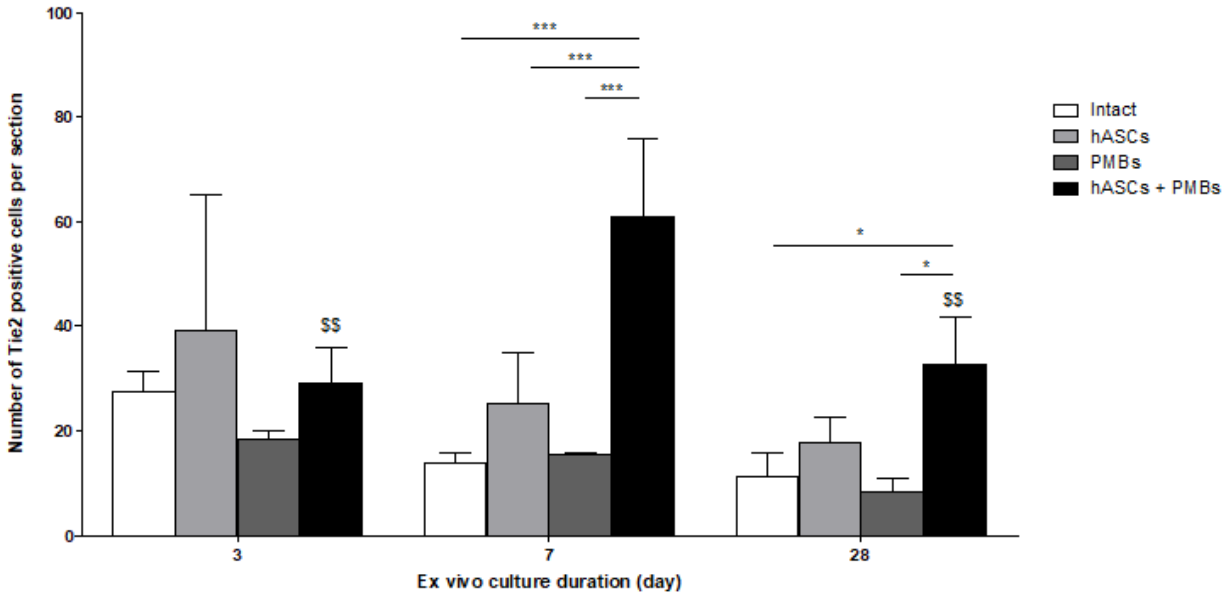

Figure S3: Quantification of Tie2-positive cells in aged-related degenerated ex vivo ovine IVDs. IVDs (n=36) were isolated from 6 sheep (3-7 years old) presenting moderate lumbar degeneration (Pfirrmann grade 2 or 3). Top cartilaginous endplates were seeded with human ASCs (n=9 discs, donors D, E and G), freshly labeled with VybrantTM DiI, and loaded PMBs with CCL5, TGF-β1 and GDF-5 (0.8 % w/w in PBS) were injected via a trans-annular injection in the NP at day 0. Control discs were either only injected with PMBs (n=9 discs), only seeded with human ASCs (n=9 discs), or 9 others kept intact (n=9 discs). After 3, 7 or 28 days of culture, IVDs were fixed with PFA 4% then coronally frozen sectioned (7 µm). Tie2+ cells were immunohistologically labeled then counted using NDP view software on high magnification stained sections. For each section, time point and donor, results are presented as the mean value of 5 measurements performed on one section. * represents a significant difference between groups, * $p<0.05$, *** $p<0.001$, two way ANOVA, Bonferroni post-test. $ represents a significant difference with the same group at day 7, $$ $p<0.01$. Abbreviations: IVD: intervertebral disc; ASCs: adipose stem cells; PMBs: pullulan microbeads; NP: nucleus pulposus; PFA: paraformaldehyde.

Table S1: Human donor information.

Donor	Age (yrs)	Gender	Experiments
A	42	Female	In vitro migration analysis
B	57	Female	In vitro migration analysis
C	64	Female	In vitro migration analysis
D	51	Female	In vitro migration analysis, ex vivo model
E	45	Female	In vitro migration analysis, ex vivo model
F	33	Female	In vitro migration analysis
G	45	Female	In vitro migration, ex vivo model

REFERENCES

[1] Abajobir AA, Abate KH, Abbafati C, Abbas KM, Abd-Allah F, Abdulkader RS, et al. Global, regional, and national disability-adjusted life-years (DALYs) for 333 diseases and injuries and healthy life expectancy (HALE) for 195 countries and territories, 1990–2016: a systematic analysis for the Global Burden of Disease Study 2016. Lancet 2017. https://doi.org/10.1016/S0140-6736(17)32130-X.

[2] Hoy D, March L, Woolf A, Blyth F, Brooks P, Smith E, et al. The global burden of neck pain: Estimates from the global burden of disease 2010 study. Ann Rheum Dis 2014;73:1309–15. https://doi.org/10.1136/annrheumdis-2013-204431.

[3] Andersson GBJ. Epidemiological features of chronic low-back pain. Lancet 1999;354:581–5. https://doi.org/http://dx.doi.org/10.1016/S0140-6736(99)01312-4.

[4] Manchikanti L, Singh V, Datta S, Cohen SP, Hirsch J a. Comprehensive review of epidemiology, scope, and impact of spinal pain. Pain Physician 2009;12:E35–70. https://doi.org/10.1016/j.jmpt.2008.08.003.

[5] Huang Y-C, Urban JPG, Luk KDK. Intervertebral disc regeneration: do nutrients lead the way? Nat Rev Rheumatol 2014;10:561–6. https://doi.org/10.1038/nrrheum.2014.91.

[6] Vergroesen PPA, Kingma I, Emanuel KS, Hoogendoorn RJW, Welting TJ, van Royen BJ, et al. Mechanics and biology in intervertebral disc degeneration: A vicious circle. Osteoarthr Cartil 2015;23:1057–70. https://doi.org/10.1016/j.joca.2015.03.028.

[7] Adams MA, Roughley PJ. What is Intervertebral Disc Degeneration, and What Causes It? Spine 2006;31:2151–61. https://doi.org/10.1097/01.brs.0000231761.73859.2c.

[8] Freemont AJ. The cellular pathobiology of the degenerate intervertebral disc and discogenic back pain. Rheumatology 2009;48:5–10. https://doi.org/10.1093/rheumatology/ken396.

[9] Walker MH, Anderson DG. Molecular basis of intervertebral disc degeneration. Spine J 2004. https://doi.org/10.1016/j.spinee.2004.07.010.

[10] Ma K, Chen S, Li Z, Deng X, Huang D, Xiong L, et al. Mechanisms of endogenous repair failure during intervertebral disc degeneration. Osteoarthr Cartil 2019;27:41–8. https://doi.org/10.1016/j.joca.2018.08.021.

[11] Clouet J, Fusellier M, Camus A, Le Visage C, Guicheux J. Intervertebral disc regeneration: From cell therapy to the development of novel bioinspired endogenous repair strategies. Adv Drug Deliv Rev 2019;146:306–24. https://doi.org/10.1016/j.addr.2018.04.017.

[12] Henry N, Clouet J, Le Bideau J, Le Visage C, Guicheux J. Innovative strategies for intervertebral disc regenerative medicine: From cell therapies to multiscale delivery systems. Biotechnol Adv 2018;36:281–94. https://doi.org/10.1016/j.biotechadv.2017.11.009.

[13] Sakai D, Andersson GBJ. Stem cell therapy for intervertebral disc regeneration: Obstacles and solutions. Nat Rev Rheumatol 2015;11:243–56. https://doi.org/10.1038/nrrheum.2015.13.

[14] Schol J, Sakai D. Cell therapy for intervertebral disc herniation and degenerative disc disease: clinical trials. Int Orthop 2019;43:1011–25. https://doi.org/10.1007/s00264-018-4223-1.

[15] Clarke LE, McConnell JC, Sherratt MJ, Derby B, Richardson SM, Hoyland JA. Growth differentiation factor 6 and transforming growth factor-beta differentially mediate mesenchymal stem cell differentiation, composition, and micromechanical properties of nucleus pulposus constructs. Arthritis Res Ther 2014;16:R67. https://doi.org/10.1186/ar4505.

[16] Xia K, Zhu J, Hua J, Gong Z, Yu C, Zhou X, et al. Intradiscal Injection of Induced Pluripotent Stem Cell-Derived Nucleus Pulposus-Like Cell-Seeded Polymeric Microspheres Promotes Rat Disc Regeneration. Stem Cells Int 2019. https://doi.org/10.1155/2019/6806540.

[17] Vadalà G, Studer RK, Sowa G, Spiezia F, Iucu C, Denaro V, et al. Coculture of bone marrow mesenchymal stem cells and nucleus pulposus cells modulate gene expression profile without cell fusion. Spine 2008;33:870–6. https://doi.org/10.1097/BRS.0b013e31816b4619.

[18] Yamamoto Y, Mochida J, Sakai D, Nakai T, Nishimura K, Kawada H, et al. Upregulation of the viability of nucleus pulposus cells by bone marrow-derived stromal cells: Significance of direct cell-to-cell contact in coculture system. Spine 2004;29:1508–14. https://doi.org/10.1097/01.BRS.0000131416.90906.20.

[19] Liang C, Li H, Tao Y, Zhou X, Li F, Chen G, et al. Responses of human adipose-derived mesenchymal stem cells to chemical microenvironment of the intervertebral disc. J Transl Med 2012. https://doi.org/10.1186/1479-5876-10-49.

[20] Sakai D, Grad S. Advancing the cellular and molecular therapy for intervertebral disc disease. Adv Drug Deliv Rev 2015;84:159–71. https://doi.org/10.1016/j.addr.2014.06.009.

[21] Vadalà G, Sowa G, Hubert M, Gilbertson LG, Denaro V, Kang JD. Mesenchymal stem cells injection in degenerated intervertebral disc: cell leakage may induce osteophyte formation. J Tissue Eng Regen Med 2012;6:348–55. https://doi.org/10.1002/term.433.

[22] Henriksson HB, Svanvik T, Jonsson M, Hagman M, Horn M, Lindahl A, et al. Transplantation of human mesenchymal stems cells into intervertebral discs in a xenogeneic porcine model. Spine 2009;34:141–8. https://doi.org/10.1097/BRS.0b013e31818f8c20.

[23] Brisby H, Papadimitriou N, Brantsing C, Bergh P, Lindahl A, Barreto Henriksson H. The Presence of Local Mesenchymal Progenitor Cells in Human Degenerated Intervertebral Discs and Possibilities to Influence These In Vitro: A Descriptive Study in Humans. Stem Cells Dev 2013;22:804–14. https://doi.org/10.1089/scd.2012.0179.

[24] Risbud M V., Guttapalli A, Tsai T-TT, Lee JY, Danielson KG, Vaccaro AR, et al. Evidence for Skeletal Progenitor Cells in the Degenerate Human Intervertebral Disc. Spine 2007;32:2537–44. https://doi.org/10.1097/BRS.0b013e318158dea6.

[25] Henriksson HB, Svala E, Skioldebrand E, Lindahl A, Brisby H. Support of Concept That Migrating Progenitor Cells From Stem Cell Niches Contribute to Normal Regeneration of the Adult Mammal Intervertebral Disc. Spine 2012;37:722–32. https://doi.org/10.1097/BRS.0b013e318231c2f7.

[26] Blanco JF, Graciani IF, Sanchez-Guijo FM, Muntión S, Hernandez-Campo P, Santamaria C, et al. Isolation and characterization of mesenchymal stromal cells from human degenerated nucleus pulposus: comparison with bone marrow mesenchymal stromal cells from the same subjects. Spine 2010;35:2259–65. https://doi.org/10.1097/BRS.0b013e3181cb8828.

[27] Gruber HE, Riley FE, Hoelscher GL, Ingram JA, Bullock L, Hanley EN. Human annulus progenitor cells: Analyses of this viable endogenous cell population. J Orthop Res 2016;2016:1351–60. https://doi.org/10.1002/jor.23319.

[28] Li X-C, Tang Y, Wu J-H, Yang P-S, Wang D-L, Ruan D-K. Characteristics and potentials of stem cells derived from human degenerated nucleus pulposus: potential for regeneration of the intervertebral disc. BMC Musculoskelet Disord 2017;18:242. https://doi.org/10.1186/s12891-017-1567-4.

[29] Wang H, Zhou Y, Chu TW, Li C-Q, Wang J, Zhang ZF, et al. Distinguishing characteristics of stem cells derived from different anatomical regions of human degenerated intervertebral discs. Eur Spine J 2016;25:2691–704. https://doi.org/10.1007/s00586-016-4522-4.

[30] Sakai D, Nakamura Y, Nakai T, Mishima T, Kato S, Grad S, et al. Exhaustion of nucleus pulposus progenitor cells with ageing and degeneration of the intervertebral disc. Nat Commun 2012;3:1264. https://doi.org/10.1038/ncomms2226.

[31] Vanden Berg-Foels WS. In situ tissue regeneration: chemoattractants for endogenous stem cell recruitment. Tissue Eng Part B Rev 2014;20:28–39. https://doi.org/10.1089/ten.TEB.2013.0100.

[32] Illien-Jünger S, Pattappa G, Peroglio M, Benneker LM, Stoddart MJ, Sakai D, et al. Homing of Mesenchymal Stem Cells in Induced Degenerative Intervertebral Discs in a Whole Organ Culture System. Spine 2012;37:1865–73. https://doi.org/10.1097/BRS.0b013e3182544a8a.

[33] Pattappa G, Peroglio M, Sakai D, Mochida J, Benneker LM, Alini M, et al. CCL5/RANTES is a key chemoattractant released by degenerative intervertebral discs in organ culture. Eur Cell Mater 2014;27:124–36; discussion 136.

[34] Honczarenko M, Le Y, Swierkowski M, Ghiran I, Glodek AM, Silberstein LE. Human bone marrow stromal cells express a distinct set of biologically functional chemokine receptors. Stem Cells 2006;24:1030–41. https://doi.org/10.1634/stemcells.2005-0319.

[35] Ponte AL, Marais E, Gallay N, Langonné A, Delorme B, Hérault O, et al. The In Vitro Migration Capacity of Human Bone Marrow Mesenchymal Stem Cells: Comparison of Chemokine and Growth Factor Chemotactic Activities. Stem Cells 2007. https://doi.org/10.1634/stemcells.2007-0054.

[36] Gruber HE, Hoelscher GL, Ingram JA, Bethea S, Norton HJ, Hanley EN. Production and expression of RANTES (CCL5) by human disc cells and modulation by IL-1-β and TNF-α in 3D culture. Exp Mol Pathol 2014. https://doi.org/10.1016/j.yexmp.2014.01.002.

[37] Wangler S, Menzel U, Li Z, Ma J, Hoppe S, Benneker LM, et al. CD146/MCAM distinguishes stem cell subpopulations with distinct migration and regenerative potential in degenerative intervertebral discs. Osteoarthr Cartil 2019;27:1094–105. https://doi.org/10.1016/j.joca.2019.04.002.

[38] Ahn SH, Cho YW, Ahn MW, Jang SH, Sohn YK, Kim HS. mRNA expression of cytokines and chemokines in herniated lumbar intervertebral discs. Spine 2002. https://doi.org/10.1097/00007632-200205010-00005.

[39] Grad S, Bow C, Karppinen J, Luk KD, Cheung KM, Alini M, et al. Systemic blood plasma CCL5 and CXCL6: Potential biomarkers for human lumbar disc degeneration. Eur Cell Mater 2016;31:1–10.

[40] Kepler CK, Markova DZ, Dibra F, Yadla S, Vaccaro AR, Risbud M V., et al. Expression and relationship of proinflammatory chemokine RANTES/CCL5 and cytokine IL-1 β in painful human intervertebral discs. Spine 2013. https://doi.org/10.1097/BRS.0b013e318285ae08.

[41] Baffi MO, Moran MA, Serra R. Tgfbr2 regulates the maintenance of boundaries in the axial skeleton. Dev Biol 2006. https://doi.org/10.1016/j.ydbio.2006.06.002.

[42] Chujo T, An HS, Akeda K, Miyamoto K, Muehleman C, Attawia M, et al. Effects of growth differentiation factor-5 on the intervertebral disc - In vitro bovine study and in vivo rabbit disc degeneration model study. Spine 2006;31:2909–17. https://doi.org/10.1097/01.brs.0000248428.22823.86.

[43] Le Maitre CL, Freemont AJ, Hoyland JA. Expression of cartilage-derived morphogenetic protein in human intervertebral discs and its effect on matrix synthesis in degenerate human nucleus pulposus cells. Arthritis Res Ther 2009;11:R137. https://doi.org/10.1186/ar2808.

[44] Park JY, Yoon YS, Park HS, Kuh SU. Molecular response of human cervical and lumbar nucleus pulposus cells from degenerated discs following cytokine treatment. Genet Mol Res 2013. https://doi.org/10.4238/2013.March.15.4.

[45] Merceron C, Portron S, Vignes-Colombeix C, Rederstorff E, Masson M, Lesoeur J, et al. Pharmacological Modulation of Human Mesenchymal Stem Cell Chondrogenesis by a Chemically Oversulfated Polysaccharide of Marine Origin: Potential Application to Cartilage Regenerative Medicine. Stem Cells 2012;30:471–80. https://doi.org/10.1002/stem.1686.

[46] Colombier P, Clouet J, Boyer C, Ruel M, Bonin G, Lesoeur J, et al. TGF-β1 and GDF5 Act Synergistically

to Drive the Differentiation of Human Adipose Stromal Cells toward Nucleus Pulposus -like Cells. Stem Cells 2016;34:653–67. https://doi.org/10.1002/stem.2249.

[47] Blanquer SBG, Grijpma DW, Poot AA. Delivery systems for the treatment of degenerated intervertebral discs. Adv Drug Deliv Rev 2015;84:172–87. https://doi.org/10.1016/j.addr.2014.10.024.

[48] Flégeau K, Pace R, Gautier H, Rethore G, Guicheux J, Le Visage C, et al. Toward the development of biomimetic injectable and macroporous biohydrogels for regenerative medicine. Adv Colloid Interface Sci 2017;247:589–609. https://doi.org/10.1016/j.cis.2017.07.012.

[49] Henry N, Clouet J, Fragale A, Griveau L, Chédeville C, Véziers J, et al. Pullulan microbeads/Si-HPMC hydrogel injectable system for the sustained delivery of GDF-5 and TGF-β1: new insight into intervertebral disc regenerative medicine. Drug Deliv 2017;24:999–1010. https://doi.org/10.1080/10717544.2017.1340362.

[50] Suffee N, Le Visage C, Hlawaty H, Aid-Launais R, Vanneaux V, Larghero J, et al. Pro-Angiogenic effect of RANTES-loaded polysaccharide-based microparticles for a mouse ischemia therapy. Sci Rep 2017. https://doi.org/10.1038/s41598-017-13444-7.

[51] Leathers TD. MINI-REVIEW Biotechnological production and applications of pullulan. Appl Microbiol Biotechnol 2003. https://doi.org/10.1007/s00253-003-l386-4.

[52] Shingel KI. Current knowledge on biosynthesis, biological activity, and chemical modification of the exopolysaccharide, pullulan. Carbohydr Res 2004;339:447–60. https://doi.org/10.1016/j.carres.2003.10.034.

[53] Cheng KC, Demirci A, Catchmark JM. Pullulan: Biosynthesis, production, and applications. Appl Microbiol Biotechnol 2011;92:29–44. https://doi.org/10.1007/s00253-011-3477-y.

[54] Pereira CL, Gonçalves RM, Peroglio M, Pattappa G, D'Este M, Eglin D, et al. The effect of hyaluronan-based delivery of stromal cell-derived factor-1 on the recruitment of MSCs in degenerating intervertebral discs. Biomaterials 2014;35:8144–53. https://doi.org/10.1016/j.biomaterials.2014.06.017.

[55] Pereira CL, Teixeira GQ, Ribeiro-Machado C, Caldeira J, Costa M, Figueiredo F, et al. Mesenchymal Stem/Stromal Cells seeded on cartilaginous endplates promote Intervertebral Disc Regeneration through Extracellular Matrix Remodeling. Sci Rep 2016;6:33836. https://doi.org/10.1038/srep33836.

[56] Leite Pereira C, Quelhas Teixeira G, Rita Ferreira J, D'Este M, Eglin D, Alini M, et al. Stromal Cell Derived Factor-1-Mediated Migration of Mesenchymal Stem Cells Enhances Collagen Type II Expression in Intervertebral Disc. Tissue Eng Part A 2018;24:1818–30. https://doi.org/10.1089/ten.tea.2018.0131.

[57] Purnama A, Aid-Launais R, Haddad O, Maire M, Mantovani D, Letourneur D, et al. Fucoidan in a 3D scaffold interacts with vascular endothelial growth factor and promotes neovascularization in mice. Drug Deliv

Transl Res 2015;5:187–97. https://doi.org/10.1007/s13346-013-0177-4.

[58] Estes BT, Diekman BO, Gimble JM, Guilak F. Isolation of adipose-derived stem cells and their induction to a chondrogenic phenotype. Nat Protoc 2010;5:1294–311. https://doi.org/10.1038/nprot.2010.81.

[59] Le Fournier L, Fusellier M, Halgand B, Lesoeur J, Gauthier O, Menei P, et al. The transpedicular surgical approach for the development of intervertebral disc targeting regenerative strategies in an ovine model. Eur Spine J 2017;26:2072–83. https://doi.org/10.1007/s00586-017-5199-z.

[60] Pfirrmann CWA, Metzdorf A, Zanetti M, Hodler J, Boos N. Magnetic resonance classification of lumbar intervertebral disc degeneration. Spine 2001;26:1873–8. https://doi.org/10.1097/00007632-200109010-00011.

[61] Illien-Junger S, Pattappa G, Peroglio M, Benneker LM, Stoddart MJ, Sakai D, et al. Homing of mesenchymal stem cells in induced degenerative intervertebral discs in a whole organ culture system. Spine (Phila Pa 1976) 2012;37:1865–73. https://doi.org/10.1097/BRS.0b013e3182544a8a.

[62] Henriksson HB, Thornemo M, Karlsson C, Hägg O, Junevik K, Lindahl A, et al. Identification of cell proliferation zones, progenitor cells and a potential stem cell niche in the intervertebral disc region: a study in four species. Spine 2009;34:2278–87. https://doi.org/10.1097/BRS.0b013e3181a95ad2.

[63] Fragkakis EM, El-Jawhari JJ, Dunsmuir RA, Millner PA, Rao AS, Henshaw KT, et al. Vertebral body versus iliac crest bone marrow as a source of multipotential stromal cells: Comparison of processing techniques, tri-lineage differentiation and application on a scaffold for spine fusion. PLoS One 2018. https://doi.org/10.1371/journal.pone.0197969.

[64] Henriksson HB, Hagman M, Horn M, Lindahl A, Brisby H. Investigation of different cell types and gel carriers for cell-based intervertebral disc therapy, in vitro and in vivo studies. J Tissue Eng Regen Med 2012;6:738–47. https://doi.org/10.1002/term.480.

[65] Henriksson HB, Papadimitriou N, Tschernitz S, Svala E, Skioldebrand E, Windahl S, et al. Indications of that migration of stem cells is influenced by the extra cellular matrix architecture in the mammalian intervertebral disk region. Tissue Cell 2015;47:439–55. https://doi.org/10.1016/j.tice.2015.08.001.

[66] Liu C, Guo Q, Li J, Wang S, Wang Y, Li B, et al. Identification of rabbit annulus fibrosus-derived stem cells. PLoS One 2014;9. https://doi.org/10.1371/journal.pone.0108239.

[67] Liu S, Liang H, Lee SM, Li Z, Zhang J, Fei Q. Isolation and identification of stem cells from degenerated human intervertebral discs and their migration characteristics. Acta Biochim Biophys Sin (Shanghai) 2017;49:101–9. https://doi.org/10.1093/abbs/gmw121.

[68] Frapin L, Clouet J, Delplace V, Fusellier M, Guicheux J, Le Visage C. Lessons learned from intervertebral disc pathophysiology to guide rational design of sequential delivery systems for therapeutic biological

factors. Adv Drug Deliv Rev 2019. https://doi.org/10.1016/j.addr.2019.08.007.

[69] Kepler CK, Ponnappan RK, Tannoury CA, Risbud M V., Anderson DG. The molecular basis of intervertebral disc degeneration. Spine J 2013;13:318–30. https://doi.org/10.1016/j.spinee.2012.12.003.

[70] Wang WJ, Yu XH, Wang C, Yang W, He WS, Zhang SJ, et al. MMPs and ADAMTSs in intervertebral disc degeneration. Clin Chim Acta 2015;448:238–46. https://doi.org/10.1016/j.cca.2015.06.023.

[71] Tran CM, Schoepflin ZR, Markova DZ, Kepler CK, Anderson DG, Shapiro IM, et al. CCN2 suppresses catabolic effects of interleukin-1beta through alpha5beta1 and alphaVbeta3 integrins in nucleus pulposus cells: implications in intervertebral disc degeneration. J Biol Chem 2014;289:7374–87. https://doi.org/10.1074/jbc.M113.526111.

[72] Wu H, Shang Y, Yu J, Zeng X, Lin J, Tu M, et al. Regenerative potential of human nucleus pulposus resident stem/progenitor cells declines with ageing and intervertebral disc degeneration. Int J Mol Med 2018. https://doi.org/10.3892/ijmm.2018.3766.

[73] Alini M, Eisenstein SM, Ito K, Little C, Kettler AA, Masuda K, et al. Are animal models useful for studying human disc disorders/degeneration? Eur Spine J 2008. https://doi.org/10.1007/s00586-007-0414-y.

[74] Nisolle J-F, Bihin B, Kirschvink N, Neveu F, Clegg P, Dugdale A, et al. Prevalence of Age-Related Changes in Ovine Lumbar Intervertebral Discs during Computed Tomography and Magnetic Resonance Imaging. Comp Med 2016;66:300–7.

[75] Tekari A, Chan SC, Sakai D, Grad S, Gantenbein B. Angiopoietin-1 receptor Tie2 distinguishes multipotent differentiation capability in bovine coccygeal nucleus pulposus cells. Stem Cell Res Ther 2016;7:75. https://doi.org/10.1186/s13287-016-0337-9.

[76] Sakai D, Schol J, Bach FC, Tekari A, Sagawa N, Nakamura Y, et al. Successful fishing for nucleus pulposus progenitor cells of the intervertebral disc across species. JOR Spine 2018. https://doi.org/10.1002/jsp2.1018.

[77] Gruber HE, Ingram JA, Norton HJ, Hanley EN. Senescence in Cells of the Aging and Degenerating Intervertebral Disc. Spine 2007. https://doi.org/10.1097/01.brs.0000253960.57051.de.

[78] Johnson WEB, Eisenstein SM, Roberts S. Cell cluster formation in degenerate lumbar intervertebral discs is associated with increased disc cell proliferation. Connect Tissue Res 2001. https://doi.org/10.3109/03008200109005650.

[79] Mohammadi E, Nassiri SM, Rahbarghazi R, Siavashi V, Araghi A. Endothelial juxtaposition of distinct adult stem cells activates angiogenesis signaling molecules in endothelial cells. Cell Tissue Res 2015. https://doi.org/10.1007/s00441-015-2228-2.

[80] Navarro A, Marín S, Riol N, Carbonell-Uberos F, Miñana MD. Human adipose tissue-resident monocytes

exhibit an endothelial-like phenotype and display angiogenic properties. Stem Cell Res Ther 2014. https://doi.org/10.1186/scrt438.

[81] Griffith JW, Sokol CL, Luster AD. Chemokines and Chemokine Receptors: Positioning Cells for Host Defense and Immunity. Annu Rev Immunol 2014;32:659–702. https://doi.org/10.1146/annurev-immunol-032713-120145.

[82] Risbud M V., Shapiro IM. Role of cytokines in intervertebral disc degeneration: pain and disc content. Nat Rev Rheumatol 2014;10:44–56. https://doi.org/10.1038/nrrheum.2013.160.

[83] Vadalà G, Russo F, Pattappa G, Schiuma D, Peroglio M, Benneker LM, et al. The Transpedicular Approach As an Alternative Route for Intervertebral Disc Regeneration. Spine 2013;38:E319–24. https://doi.org/10.1097/BRS.0b013e318285bc4a.